1968

Carbon-13 Isotope Effects In Nucleophilic Substitution Reactions

Anthony James Mcnamara

CARBON-13 ISOTOPE EFFECTS IN NUCLEOPHILIC SUBSTITUTION REACTIONS

by

Anthony James McNamara

Department of Chemistry

Submitted in partial fulfillment

of the requirements for the degree of

Doctor of Philosophy

Faculty of Graduate Studies

The University of Western Ontario

London, Canada.

April 1968

ABSTRACT

Carbon-13 kinetic isotope effects, k^{12}/k^{13}, were measured for the reaction of benzyl, p-chlorobenzyl, and p-methylbenzyl chlorides with ethoxide and/or methoxide ion. The Badger rule and the Bigeleisen γ approximation were used to calculate k^{12}/k^{13} values for two-parameter models for the transition state of this reaction. Reasonable models gave calculated values in good agreement with observation. Calculation of the substituent effect on k^{12}/k^{13} using the Swain-Thornton rule, however, led to predictions opposite to those observed. It is proposed that resonance interaction with the ring is involved, and that a two-parameter model is therefore inadequate.

Techniques were developed for the separation and degradation of the reaction products. A modification of the Schmidt decarboxylation was evolved and tested, thus greatly widening the scope of this reaction for both degradative and preparative applications.

k^{12}/k^{13} measurements were made on the α-toluenesulphonyl bromide-bromide ion reaction for Prof. J.F. King and Dr. D.J.H. Smith. The results were consistent with their mechanism. The substituent effect paralleled that found for the benzyl chloride-alkoxide ion reaction.

ACKNOWLEDGMENTS

The author gratefully acknowledges the guidance provided throughout this work by his faculty advisor, Prof. J.B. Stothers.

Thanks is also due the many staff members who made their facilities available when needed; in particular the author's thanks go to Prof. H.W. Baldwin for the frequent use made of his mass spectrometer.

Financial assistance in the form of two fellowships from Canadian Industries Limited (1962-3, 1963-4) was most helpful and is much appreciated.

Lastly, the author would like to thank a faculty member and long-time friend, Prof. W.C. ''Pete'' Howell for the personal encouragement he gave all along the way.

TABLE OF CONTENTS

LIST OF TABLES

LIST OF FIGURES

CHAPTER I

INTRODUCTION

A. General

The cornerstone of modern reaction mechanism theory is the concept of the transition state.

From the moment the reactants begin the process of transforming themselves into products until those products appear as such, no fixed structure exists. All that does exist during that period is a constantly changing assemblage of atoms, no configuration of which has any finite lifetime.

The transition state is the structure one would observe if it were somehow possible to 'freeze' the assemblage at the configuration that 'exists' at the point of highest energy on the reaction coordinate linking products and reactants.

Obviously, then, transition states cannot be examined as such, and their 'structures' must be inferred from indirect measurements.

The component parts of a transition state are revealed by an investigation of the molecularity of the reaction, and the spatial relationship of those components by a study of the stereochemistry of the reaction. But quantitative information in regard to such things as 'bond' lengths is difficult to obtain.

The Eyring transition state theory can, in principle, reveal the intimate details of transition state 'structure'; in practice, however, it requires quantitative data of a type which is not at present obtainable.

Kinetic isotope effect theory, on the other hand, appears to offer hope that the goal can be reached.

As things now stand, kinetic isotope effect theory is capable of predicting an isotope effect for a given transition state 'structure' with some accuracy it would seem. Unfortunately, however, it yields, for a given kinetic isotope effect, not a single transition state 'structure' but rather, a series of such 'structures' without, at the same time providing a way of choosing from among the members.

It was hoped, at the outset of the work reported here, that the magnitude and direction of the substituent effect on the kinetic isotope effect, combined with what is known

about substituent effects in other regards, would allow a firm choice from among the members of whatever series was predicted by the kinetic isotope effect theory.

B. Isotope Effects

1. Pioneer work

The first clear recognition of isotopes as chemically indistinguishable substances was due to McCoy and Ross (1). The term 'isotope' was coined by Soddy, whose brilliant elucidation of the chemistry of mesothorium 1 led him to his theory of radioactive isotopes (2), for which he was awarded the Nobel Prize in 1921.

Although it was realized almost immediately by many workers that isotopes of a given element should undergo identical chemical reactions but should do so at different rates, nearly a decade passed before Lindeman (3,4) made the first, albeit unsuccessful, attempt at demonstrating an isotope effect. His efforts failed because of the very small relative mass difference between the isotopes of the heavy elements he was forced to employ, for the minute isotope effects associated with such small mass differences were not detectable by his measuring techniques.

It was not until the isotopes of the lighter elements deuterium (5,6), carbon (7), nitrogen (8,9) and oxygen (10,11) were discovered that the study of this phenomenon became practicable.

The first successful demonstration of an isotope effect was carried out by Urey (5), who predicted, on the basis of statistical-mechanical calculations, a significant difference in the vapour pressures of deuterium hydride and hydrogen, and effected a separation of these two compounds by fractional distillation.

The first demonstration of a kinetic isotope effect is credited to Washburn and Urey, who in 1932 observed deuterium enrichment in the liquid phase during the electrolysis of water (12).

2. Isotope exchange reactions

In 1933 Urey (13) predicted the equilibrium constant for the isotope exchange reaction

$$H_2 + D_2 \rightleftharpoons 2HD$$

A year later it was shown (14) that his predicted value was correct. Subsequently, a series of his predicted equilibrium constants for simple exchange reactions involving isotopes of the light elements hydrogen, lithium, carbon and nitrogen received experimental verification (15,16,17).

More recently, Bigeleisen (18) has developed a general equation for the prediction of such equilibrium constants.

His method requires only a knowledge of the infrared vibrational frequencies of the molecular species involved in the equilibrium. An illustrative example of the use of the Bigeleisen theory in this way is given in Wiberg's text on physical organic chemistry (19) for the reaction

$$CH_4 + DBr \rightleftharpoons CH_3D + HBr$$

3. Kinetic isotope effects

a. General

The kinetic isotope effect is defined as the ratio, for a given reaction, of the rate constants for the 'normal' and for the isotopically-substituted reactants. Thus for the paired reactions represented by equations 1 and 2,

$$M + N \xrightarrow{k} \text{products} \qquad (1)$$

$$M' + N \xrightarrow{k'} \text{products} \qquad (2)$$

in which M and M' represent different isotopic species, the kinetic isotope effect is k/k'. The mass numbers of the isotopes involved are attached, as superscripts, to the rate constants; for example, a carbon-13 kinetic isotope effect is indicated by the expression k^{12}/k^{13}. (North American usage is such that k' refers to the

reaction of the molecule containing the heavier isotope; it should be noted that much data in the older literature, however, as well as that reported in current European publications, employs the reverse convention.)

Two general types of kinetic isotope effects are recognized, 'primary' and 'secondary'. This distinction is a mechanistic one, i.e. it is made on the basis of whether or not a bond(s) directly involving the isotope in question is (are) broken and/or formed in the reaction. If such bond rupture and/or formation is involved, the kinetic isotope effect observed is a primary one. On the other hand, a kinetic isotope effect may be observed even though no such bond rupture and/or formation occurs at any time during the reaction; the effect in this case is described as being a secondary one. Secondary kinetic isotope effects are orders of magnitude smaller than primary ones, and very few have been observed for isotopes of elements other than hydrogen.

b. Theoretical treatments

i. Introduction

Various theoretical approaches to an understanding of kinetic isotope effects have been moderately successful for certain well-defined reactions including a number of

unimolecular thermal decompositons, proton transfer reactions and electrophilic displacements. All these treatments have a common foundation in the transition-state theory of chemical kinetics.

This, the Eyring theory (20), proposes that the reactants are involved in a (quasi)-equilibrium with a so-called 'transition-state' or 'activated complex', and that the rate-controlling step of the overall reaction is the decomposition of this complex to products. The rate of the reaction is therefore dependent on the 'concentration' of the transition state.

The transition state differs fundamentally from an ordinary stable molecular species in that it lacks one vibrational mode. The 'missing' mode is replaced by a translational mode along the reaction coordinate.

Since the rate constant, k, depends on $K^{\ddagger}$, the equilibrium constant for the equilibrium between the transition state and the reactants, the reaction rate can be considered in terms of $\Delta F^{\ddagger}$, the free energy of activation.

The general situation for the processes corresponding to Equations 1 and 2 is illustrated in Fig. 1.

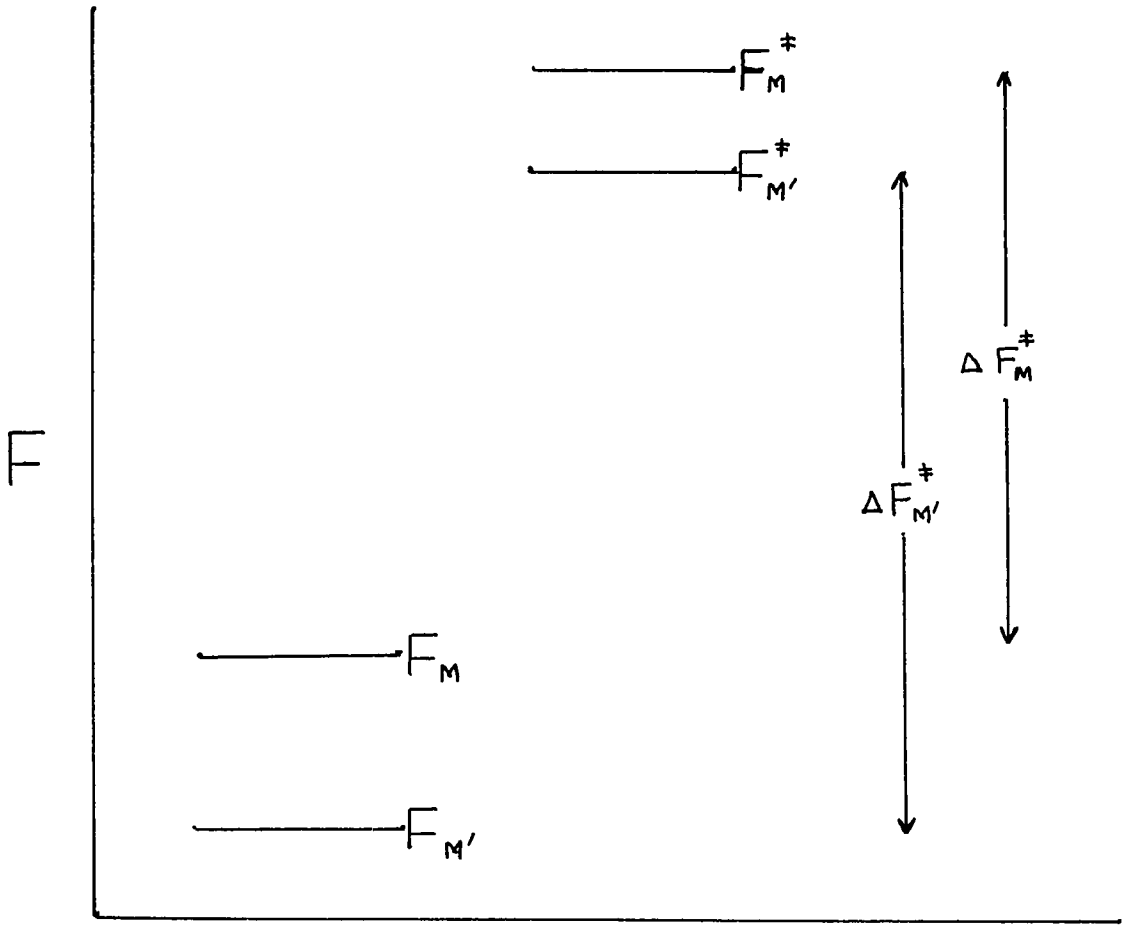

Figure 1

If $\Delta F_M^{\ddagger} = \Delta F_{M'}^{\ddagger}$, $k = k'$, $k/k' = 1.000$, and no kinetic isotope effect is observed. If $\Delta F_M^{\ddagger} \neq \Delta F_M^{\ddagger}$, $k \neq k'$, and an isotope effect is observed.

In a simple though crude treatment, kinetic isotope effects have been assumed to arise solely from changes in a single vibrational mode. This approach (21) has been surprisingly effective for the prediction of the magnitude of the deuterium isotope effect, k^H/k^D, in processes involving carbon-hydrogen bond ruptures. It is assumed for this approximation that all vibrational modes of the reactant molecule are independent of one another. It is then possible to describe the vibrational energy of a molecule, MH, as

$$E_{MH} = A + \tfrac{1}{2}h\nu_H \qquad (3)$$

where $\tfrac{1}{2}h\nu_H$ is the zero-point energy of the carbon-hydrogen bond and A is the sum of the contributions of all the other vibrational modes.

Similarly, for the molecule, MD,

$$E_{MD} = A + \tfrac{1}{2}h\nu_D \qquad (4)$$

where $\tfrac{1}{2}h\nu_D$ is the zero-point energy of the carbon-deuterium bond.

For the corresponding transition states, it follows that

$$E^{\ddagger}_{MH} = A + \tfrac{1}{2}h\nu^{\ddagger}_{H} \qquad (5)$$

and

$$E^{\ddagger}_{MD} = A + \tfrac{1}{2}h\nu^{\ddagger}_{D} \qquad (6)$$

If it is further assumed that complete bond rupture has occurred in the transition state, $\nu^{\ddagger}_{H}$ and $\nu^{\ddagger}_{D}$ are zero, and $E^{\ddagger}_{MH} = E^{\ddagger}_{MD}$. Thus

$$\Delta(\Delta F^{\ddagger}) = \Delta F^{\ddagger}_{MH} - \Delta F^{\ddagger}_{MD} \qquad (7)$$

The rate difference is then governed only by the difference between the zero-point energies of the reactants. Typical zero-point energies are 4.15 kcal/mole for a carbon-hydrogen bond and 3.00 for a carbon-deuterium bond. The difference, 1.15 kcal/mole, corresponds to a rate ratio, or k_H/k_D, of about seven, a value closely approximated in many reactions involving carbon-hydrogen bond cleavages.

This very simple treatment is limited in its effectiveness to primary kinetic isotope effects associated with the isotopes of hydrogen.

ii. The Bigeleisen equations

A vastly more sophisticated theoretical treatment

than that just described is needed for the prediction and interpretation of the isotope effects associated with the isotopes of elements heavier than those of hydrogen. Such a treatment is the widely-accepted one due to Bigeleisen.

A detailed development of the Bigeleisen equations is given in Appendix B of this thesis; only an outline of that development is described here.

Transition-state theory postulates the existence of a quasi-equilibrium between the transition state and the reactants. For the reaction described by Equation 8

$$1 + B \xrightarrow{k_1} \text{products} \qquad (8)$$

the equilibrium constant, $K_1^{\ddagger}$, for the quasi-equilibrium is given, in terms of partition functions, by Equation 9

$$K_1^{\ddagger} = \frac{Q_1^{\ddagger}}{Q_1 \, Q_B} \qquad (9)$$

For the parallel reaction

$$2 + B \xrightarrow{k_2} \text{products} \qquad (10)$$

in which reactant 2 is the same as reactant 1 except in its isotopic composition,

$$K_2^{\ddagger} = \frac{Q_2^{\ddagger}}{Q_2 \, Q_B} \qquad (11)$$

It follows then that the ratio of the rate constants, i.e. the kinetic isotope effect, is

$$\frac{k_1}{k_2} = \frac{Q_2 \, Q_1^{\ddagger}}{Q_1 \, Q_2^{\ddagger}} \tag{12}$$

To a good approximation, the total partition function, Q, is equal to the product of the individual partition functions Q_t (translational), Q_v (vibrational), Q_r (rotational), and Q_e (electronic):

$$Q = Q_t \cdot Q_v \cdot Q_r \cdot Q_e \tag{13}$$

For the case of a non-linear molecule in its electronic ground state,

$$\frac{Q_2}{Q_1} = \frac{S_2}{S_1}\left[\frac{M_2}{M_1}\right]^{3/2}\left[\frac{I_{A_2} I_{B_2} I_{C_2}}{I_{A_1} I_{B_1} I_{C_1}}\right]\prod_i e^{\frac{hc(\nu_{1i}-\nu_{2i})}{2\kappa T}} \frac{1 - e^{-\frac{hc\nu_{1i}}{\kappa T}}}{1 - e^{-\frac{hc\nu_{2i}}{\kappa T}}} \tag{14}$$

Application of either the Teller-Redlich product rule or the high-temperature limit to Equation 14 leads to Equation 15:

$$\prod_{j}^{n}\left[\frac{m_{1_j}}{m_{2_j}}\right]^{3/2}\frac{Q_2 S_2}{Q_1 S_1} = \prod_{i}^{3n-6}\left[\frac{\nu_{2i}}{\nu_{1i}}\, e^{\frac{hc(\nu_{1i}-\nu_{2i})}{2\kappa T}}\, \frac{1 - e^{\frac{-hc\nu_{1i}}{\kappa T}}}{1 - e^{\frac{-hc\nu_{2i}}{\kappa T}}}\right] \tag{15}$$

If f is defined as

$$f = \prod_{j}^{n}\left[\frac{m_{1_j}}{m_{2_j}}\right]\frac{Q_2}{Q_1} \tag{16}$$

and u_i defined as

$$u_i = \frac{hc\nu_i}{\kappa T} \tag{17}$$

and

$$u_{1_i} = u_{2i} + \Delta u_i \tag{18}$$

Equation 15 becomes

$$\frac{S_2}{S_1} f = \prod_{i}^{3n-6}\left[\frac{u_i}{u_i + \Delta u_i}\, e^{\frac{\Delta u_i}{2}}\, \frac{1 - e^{-(u_i + \Delta u_i)}}{1 - e^{-u_i}}\right] \tag{19}$$

Taking logarithms of both sides converts Equation 19 into Equation 20:

$$\ln f + \ln \frac{S_2}{S_1} = \sum_i^{3n-6} \left[\ln \frac{u_i}{u_i + \Delta u_i} + \frac{\Delta u_i}{2} + \ln \frac{1 - \ell^{-(u_i + \Delta u_i)}}{1 - \ell^{-u_i}} \right] \tag{20}$$

For all cases in which $\Delta u_i \ll 1$, i.e. all cases except those involving the isotopes of hydrogen, Equation 20 becomes

$$\ln f + \ln \frac{S_2}{S_1} = \sum_i^{3n-6} G(u_i) \Delta u_i \tag{21}$$

$$\text{where } G(u_i) = \frac{1}{2} - \frac{1}{u_i} + \frac{1}{\ell^{u} - 1}$$

and thus

$$\frac{S_2}{S_1} f = 1 + \sum_i^{3n-6} G(u_i) \Delta u_i \tag{22}$$

In a manner analogous to that used in the development of Equation 22, it can be shown that

$$\frac{S_2^{\ddagger}}{S_1^{\ddagger}} f = \frac{\nu_{1_L}^{\ddagger}}{\nu_{2_L}^{\ddagger}} \left[1 + \sum_i^{3n-7} G(u_i^{\ddagger}) \Delta u_i^{\ddagger} \right] \tag{23}$$

for the transition state.

It follows then that

$$\frac{k_1\ S_2\ S_1^{\ddagger}}{k_2\ S_1\ S_2^{\ddagger}} = \frac{\nu_{1L}^{\ddagger}}{\nu_{2L}^{\ddagger}} \left[1 + \sum_i^{3n-6} G(u_i)\,\Delta u_i - \sum_i^{3n-7} G(u_i^{\ddagger})\,\Delta u_i^{\ddagger} \right] \quad (24)$$

Equation 24 is Bigeleisen's 'G of u' equation.

Another important Bigeleisen equation, the so-called 'gamma-bar approximation' may be developed as follows:

Expansion of G(u) in powers of u gives u/12 as the leading term. For small values of u_i and Δu_i, Equation 22 can be rewritten

$$\frac{S_2}{S_1}\left\{ = 1 + \sum_i^{3n-6} \frac{u_i}{12}\,\Delta u_i \right. \quad (25)$$

$$= 1 + \sum_i^{3n-6} \frac{u_{1i}^2 - u_{2i}^2}{24} \quad (26)$$

Application of the sum rule to Equation 26 gives

$$\frac{S_2}{S_1}\left\{ = 1 + \frac{1}{24}\left[\frac{\hbar c}{\kappa T}\right]^2 \sum_j^{3n} \left[\frac{1}{m_{1j}} - \frac{1}{m_{2j}}\right] a_{jj} \right. \quad (27)$$

The 'second quantum correction' is introduced in the following way:

Equation 22 can be rewritten:

$$\frac{S_2}{S_1}f = 1 + \sum_{i}^{3n-6} G(u_i)\,\Delta u_i \frac{12u_i}{12u_i} \tag{28}$$

$$1 + \sum_{i}^{3n-6} \gamma_i \frac{u_i}{12}\,\Delta u_i \tag{29}$$

$$\text{where } \gamma_i = \frac{12G(u_i)}{u_i}$$

$$\frac{S_2}{S_1}f = 1 + \sum_{i}^{3n-6} \frac{\gamma_i}{24}\left[u_{1_i}^2 - u_{2_i}^2\right] \tag{30}$$

Because γ_i is somewhat insensitive to changes in u_i, it is possible to define a quantity $\bar{\gamma}$ such that

$$\frac{S_2}{S_1}f = 1 + \bar{\gamma} \sum_{i}^{3n-6} \frac{u_{1_i}^2 - u_{2_i}^2}{24} \tag{31}$$

Equation 27 can now be modified:

$$\frac{S_2}{S_1}f = 1 + \frac{1}{24}\left[\frac{\not{\kappa}c}{T}\right]^2 \bar{\gamma} \sum_{j}^{3n} \left[\frac{1}{m_{1_j}} - \frac{1}{m_{2_j}}\right] a_{jj} \tag{32}$$

It can be shown that Equation 23 is equivalent to Equation 33:

$$\frac{k_1\ S_2\ S_1^{\ddagger}}{k_2\ S_1\ S_2^{\ddagger}} = \frac{\nu_{1_L}^{*}}{\nu_{2_L}^{*}}\left[1 + \sum_{i}^{3n-6} G(u_i)\Delta u_i - \sum_{i}^{3n-6} G(u_i^{\ddagger})\Delta u_i^{\ddagger}\right] \qquad (33)$$

By the above sequence of transformations, Equation 33 becomes Equation 34:

$$\frac{k_1\ S_2\ S_1^{\ddagger}}{k_2\ S_1\ S_2^{\ddagger}} = \frac{\nu_{1_L}^{*}}{\nu_{2_L}^{*}}\left[1 + \frac{\bar{\gamma}}{24}\sum_{i}^{3n-6}\left(u_{1_i} - u_{2_i}\right) - \frac{\bar{\gamma}^{\ddagger}}{24}\sum_{i}^{3n-6}\left(u_{1_i}^{\ddagger} - u_{2_i}^{\ddagger}\right)\right] \qquad (34)$$

and if $\bar{\gamma} \doteqdot \bar{\gamma}^{\ddagger}$,

$$\frac{k_1\ S_2\ S_1^{\ddagger}}{k_2\ S_1\ S_2^{\ddagger}} = \frac{\nu_{1_L}^{*}}{\nu_{2_L}^{*}}\left[1 + \frac{\bar{\gamma}}{24}\left[\frac{\hbar c}{\kappa T}\right]^2 \sum_{j}^{3n}\left[\frac{1}{m_{1_j}} - \frac{1}{m_{2_j}}\right]\left[a_{jj} - a_{jj}^{\ddagger}\right]\right] \qquad (35)$$

Equation 35 is the 'gamma-bar approximation'.

C. Nucleophilic Substitution Reactions

1. General

The term, nucleophilic substitution reaction, refers to that multitude of reactions whose stoichiometry is described by the general equation,

$$R_3C\text{-}X + Y^- \longrightarrow Y\text{-}CR_3 + X^-$$

in which the nucleophile, Y^-, possesses an unshared electron pair with which it forms the C-Y bond in the product. Y may be an anion or a neutral molecule. X^-, the leaving group, gains sole possession of the electron pair of the original C-X bond as this bond ruptures.

In their now classic series of papers beginning in 1933, Hughes and Ingold (22) developed the concept of a duality of mechanism for nucleophilic substitution reactions, coining, in the process, the terms S_N1 and S_N2 to describe and identify two extreme mechanisms (23).

The S_N1 process, often called the 'two-step' or 'carbonium ion' mechanism, involves a preliminary and rate-controlling heterolysis of the C-X bond to yield an intermediate cation or carbonium ion. This ion subsequently combines with a nucleophile to form product, or recombines with X^- to return to starting material. The

process is described by Equations

$$RX \underset{k_{-1}}{\overset{k_1}{\rightleftharpoons}} R^+ + X^-$$

$$R^+ + Y^- \xrightarrow{k_2} \text{product}$$

Although in many systems the observed rate of an S_N1 reaction is simply first-order in R-X and zero-order in Y^-, i.e.

$$\text{rate} = k_1[RX]$$

more complex rate expressions can arise depending on the relative magnitudes of k_1, k_{-1} and k_2. A more generally applicable expression based on the steady-state approximation is Equation

$$\text{rate} = \frac{k_1 k_2 [RX][Y^-]}{k_2[Y^-]+k_{-1}[X^-]}$$

The S_N2 process, often called the 'synchronous' or 'bimolecular' mechanism involves but a single step, one in which the R-Y bond is formed by the attack of the nucleophile, Y, with its unshared electron pair, while, simultaneously, the R-X bond is ruptured. The process is thus clearly bimolecular and the rate first-order in both substrate and nucleophile. The rate expression is then

$$\text{rate} = k_2[RX][Y^-]$$

Of course, in those cases in which [Y] $\gg$ [RX], for instance in solvolyses, pseudo-first-order kinetics are observed:

$$\text{rate} = (k_2[Y])[RX]$$

$$= k_2' [RX]$$

Many nucleophilic substitution reactions exhibit 'mixed-order' kinetics, i.e. orders between one and two, and reference is often made in this regard to mechanisms 'intermediate between S_N1 and S_N2'. Much controversy has arisen over this point, and agreement on the subject is still far from unanimous. Purists insist that, because the terms S_N1 and S_N2 describe the molecularity of the rate-controlling step of the reaction, and because there either is or is not a molecule of the nucleophile in the transition state for that step, the molecularity must, of course, be integral, and the mechanism either S_N1 or S_N2 (24). Others, less concerned with semantics, feel that a whole series of transition states ranging in 'structure' all the way from purely S_N1 to purely S_N2 is possible, and find it convenient to discuss its members in terms of their S_N1- or S_N2-like character. The whole problem is the result of the fact that reaction mechanisms are

described in terms of molecularities while kinetic measurements yield reaction orders.

2. The S_N2 Mechanism

The S_N2 process involves an attack on the carbon atom bearing the X group by the nucleophile, with concomitant rupture of the C-X bond, the nucleophile, in effect, 'pushing off' the leaving group.

The carbon atom being substituted is attacked from the side opposite to that at which the group to be displaced is attached; a Walden inversion (25,26) results, i.e. the center at which substitution takes place suffers stereochemical inversion. This phenomenon is illustrated in Figure 2.

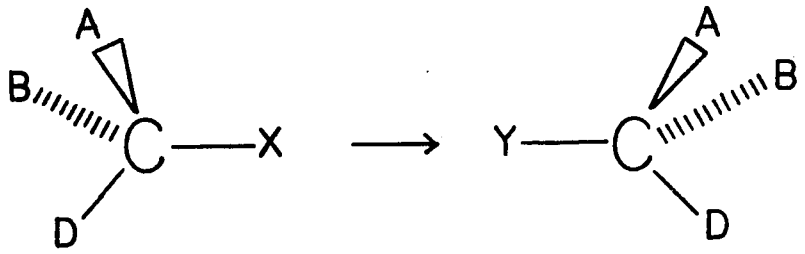

Figure 2

Hughes (27) compared the rates of substitution and racemization of optically active 2-iodooctane when this compound was allowed to react with radioactive iodide ion. The observed rates were identical, showing that each act

of substitution resulted in an inversion. This and similar studies using optically active 1-bromo-1-phenylethane (27) and 2-bromopropionic acid (28) led Hughes and Ingold to conclude that 'bimolecular substitutions are invariably accompanied by steric inversion'. (29)

It might be noted that this phenomenon of backside attack cannot be due to coulombic forces (e.g. repulsion between an attacking anion and a negative leaving group), for if such were the case, frontside rather than the observed backside attack would have been found in such reactions as the acetolysis of D(+)-1-phenethyltrimethyl-ammonium ion (30) and the reaction between bromide ion and the dimethyl(α-methylbenzyl)sulphonium ion (31).

Since the S_N2 reaction is bimolecular and involves inversion, it is apparent that during the course of the reaction a 'structure' such as I must be formed. The carbon atom constituting the reaction site becomes temporarily pentavalent and its configuration trigonal bipyramidal; the C-X and C-Y 'bonds' are both longer and weaker than normal C-X and C-Y covalent bonds, and, although of equivalent strength, i.e. having equal force constants, are not necessarily equivalent in length.

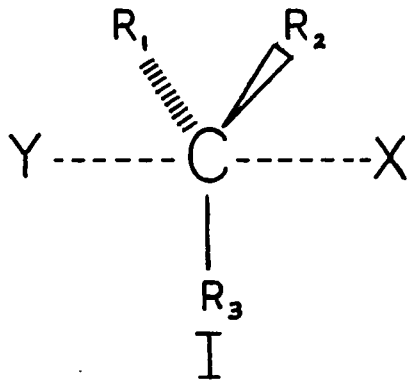

Figure 3

Structure I is generally considered to represent the S_N2 transition state, although it should be borne in mind that I may be a highly reactive reaction intermediate (32).

Some impression, even an intuitive one, of the 'structure' of the transition state is required for a consideration of the kinetic isotope effect for a given process. To this end, two qualitative postulates for the prediction of transition state 'structures' are valuable. One of these postulates is due to Hammond (33), the other to Swain and Thornton (34).

The Hammond postulate relates the geometry of the transition state to the relative energy contents of the reactants, the transition state, and the products of the reaction:

If two states, as for example, a transition state and an unstable intermediate, occur consecutively during a reaction process and have nearly the same energy content,

their interconversion will involve only a small reorganization of the molecular structures .

Only three species occur along the reaction coordinate in the case of an S_N2 reaction: the reactants, the transition state, and the products. The Hammond postulate, then, predicts that the transition state for either highly exothermic or endothermic reactions will more closely resemble whichever of the other two species, the reactants or the products, it more nearly equals in energy content.

In the case of a highly exothermic reaction, i.e. one for which

$$E_{reactants} \gg E_{products}$$

it follows that

$$E_{transition\ state}-E_{reactants} \ll E_{transition\ state}-E_{products}$$

Since the transition state in this instance is much nearer in energy content to the reactants than to the products, it is postulated that the transition state is reactant-like.

Conversely, in the case of a highly endothermic reaction, i.e. one for which

$$E_{reactants} \ll E_{products}$$

and therefore

$E_{\text{transition state}} - E_{\text{reactants}} \gg E_{\text{transition state}} - E_{\text{products}}$

Hammond proposes a product-like transition state.

For reactions which are neither highly endothermic nor highly exothermic, the Hammond postulate makes no prediction as to their transition state geometry other than to suggest that neither the reactants nor the products are likely to be good models.

Energy profiles illustrative of this postulate are shown in Figure 4.

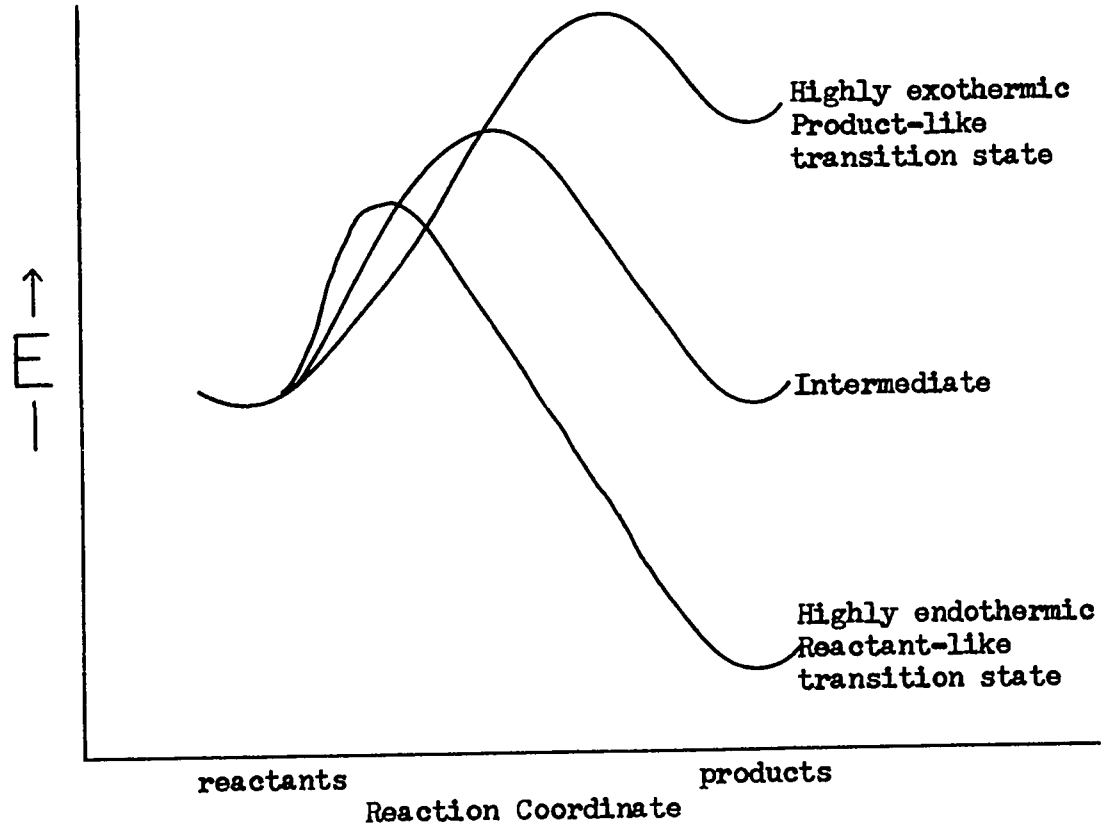

Figure 4

The Hammond postulate cannot be used with any confidence for a comparison of transition states for reactions which differ from each other only in the identity of a substituent in one of the reactants, because a change in a substituent rarely causes any great change in the heat of reaction.

On the other hand, it is to just such cases, in displacement reactions, that the proposals put forth by Swain and Thornton are applicable.

For the interpretation of substituent effects on the transition state for the three-center reaction, these authors consider two general cases, one in which no π-overlap occurs at the reaction center, the other in which π-overlap does occur.

The first of these postulates, the so-called 'Swain-Thornton rule' states that (35):

Electron-supplying substituents tend to lengthen transition state bonds which are being made or broken .

For the general reaction

$$Y + C\text{-}X \longrightarrow [Y\text{-----}C\text{-----}X] \longrightarrow Y\text{-}C + X$$

the 'rule' predicts that the introduction of an electron-donating substituent into Y will lengthen the Y----C 'bond'

and shorten the C----X 'bond' in the transition state, where such a substitution into X will have just the opposite effect. An electron-donating substituent so introduced into C will lengthen both the Y--- C and C---X 'bonds'.

It follows, of course, that an electron-withdrawing substituent would have the reverse effect in each of the above cases.

When π-systems are present and are able to interact conjugatively with any of the transition state 'bonds', the Swain-Thornton rule is somewhat modified, and is applied in accordance with the following prescription:

In a simple atomic orbital diagram of the transition state, locate all 'reacting bonds', bonds which are present in the transition state but entirely absent in either reactants (for bonds being made) or products (for bonds being broken). A 'reacting orbital' defines an electron cloud, bounded by nuclei but containing no nuclei, which includes one reacting bond. Identify the reacting orbitals, each composed of the atomic orbital portions of a reacting bond plus all other atomic orbital portions which overlap them at the transition state, each portion bounded by nuclei but with no interposed nuclei; i.e. halves of a p- or s-orbital belong to different reacting orbitals. Starting at the point of structure

change, star (*) the nearest reacting orbital(s) and alternate more remote reacting orbitals. Wavemark (~) other reacting orbitals. The rule is that bonds utilizing starred orbitals are lengthened by electron-supplying substituents and shortened by electron-attracting substituents; the opposite is true for bonds utilizing waved orbitals .

The transition state of the benzyl chloride-methoxide ion reaction is illustrated in Figure 5, and the Swain-Thornton 'starred-wavemarked' diagram in Figure 6.

Both the C----O and the C----Cl 'bonds' are starred in the Swain-Thornton diagram, and the rule predicts that both will be lengthened by the p-substituent, X, if it be electron-donating in character. In addition, the C_1-C_α bond will be shortened under these circumstances.

Thornton has recently reexamined the Swain-Thornton postulate, and reasserted its validity (36).

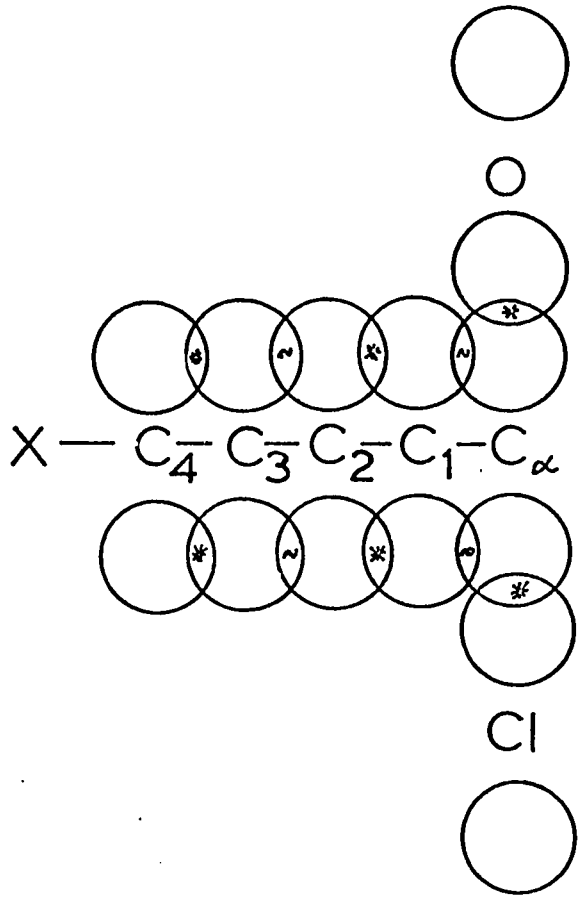

Figure 5

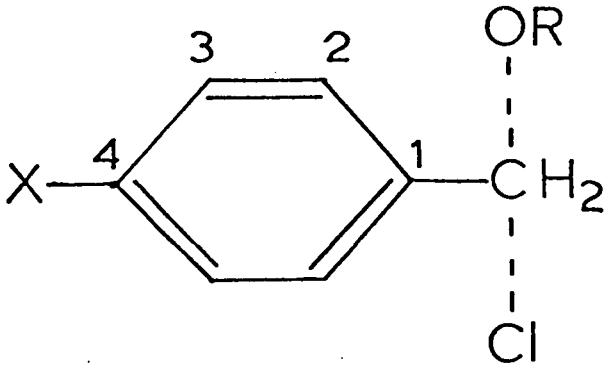

Figure 6

CHAPTER II

EXPERIMENTAL

A. Introduction

Natural-abundance materials were used throughout this work in the determination of the carbon-13 kinetic isotope effects. The carbon atom at the reaction site thus being naturally labelled with carbon-13 to the extent of about 1.1%, no artificial enrichment of starting materials was required.

The isotopic abundance ($^{12}C/^{13}C$) at the reaction center of the product relative to that of the corresponding position in the starting material is a function of the extent to which the reaction has progressed, the difference between these two isotopic abundances being a maximum at the very beginning of the reaction, and zero at the end.

The ratio of the reaction-center isotopic abundance of the very first increment of product to that of the reaction-center of the original starting material is the kinetic isotope effect, k^{12}/k^{13}. Since, in practice, the

reaction must be allowed to proceed far enough to permit isolation, purification, and isotopic analysis of the product, the observed ratio is, of course, less than maximal. The kinetic isotope effect can be related to the observed ratio using a knowledge of the degree of completion of reaction, by means of an equation developed by Stevens and Attree (37):

$$\frac{k^{12}}{k^{13}} = \frac{\ln(1-f)}{\ln(1-\frac{f}{r})}$$

where f = fraction reacted

r = observed ratio of isotopic abundances

Two substitution reactions were studied in this work, the first being the reaction of a benzyl chloride with an alkoxide ion, and the second the reaction of an α-toluenesulphonyl bromide with bromide ion.

1. The Alkoxide-ion-Benzyl Chloride Reaction

Kinetic measurements were made for these reactions, and the rate-constants obtained used to determine suitable reaction times.

Each isotope effect run was quenched by the addition of excess dilute aqueous alkali at a time such as to give about 10% reaction. Ether extraction followed by solvent

removal gave an ether-soluble mixture of unreacted starting material and reaction product in the ratio of about 9 to 1.

Various methods were used in isolating from such mixtures the reaction products completely free of unreacted starting materials. Trial separations were made on synthetic mixtures, but the ultimate test of a technique was always the magnitude of the mean deviation of the kinetic isotope effect for an actual isotope effect triplicate run. The development of these techniques was thus very slow.

Gas-liquid chromatography was used for all the benzyl chloride runs (methoxide, ethoxide, and methanol). Excellent separations were obtained on analytical columns packed with diethylene glycol succinate on Chromosorb P. An early attempt to use $^{3}/_{8}$ inch columns on an analytical machine failed, however, when decomposition of benzyl chloride in the detector block led, on repeated sample injection, to blockage of the gas passages. A Nestor-Faust Prepko I preparative unit was then tested. Adequate separations were obtainable provided that sample injections were kept small, but an unacceptable scatter was observed when actual runs were made. This scatter decreased to acceptable proportions only after both the metal column and the stainless steel preheater unit were replaced with glass components.

The higher operating temperatures required plus the greater reactivity of the substituted benzyl chlorides ruled out the use of g.l.c. for any but the unsubstituted series.

In the case of p-chlorobenzyl chloride the reaction mixture was hydrolyzed in aqueous alkali. On cooling, the bulk of the p-chlorobenzyl alcohol so produced was removed mechanically after it had crystallized. Low-boiling petroleum ether was used to crystallize out further quantities of the alcohol, and the last traces were removed on activated alumina.

p-Methylbenzyl methyl ether and p-methylbenzyl chloride were largely separated by fractional distillation; the impure ether thus obtained was refluxed with aqueous alkali to hydrolyze the remaining chloride, and the resulting alcohol removed by subsequent chromatography on activated alumina.

No attempt was made to realize quantitative isolation of the benzyl ethers, the major effort being devoted in this separation to their obtention completely free from starting materials and/or hydrolysis products.

Oxidation of the starting materials to benzoic acids, the first step towards determining the isotopic abundances at their reaction centers, was quite straightforward in

the case of both benzyl and p-chlorobenzyl chloride, alkaline permanganate giving satisfactory results in both cases. On the other hand, since p-methylbenzyl chloride gives terephthalic acid on permanganate oxidation, and either unsatisfactory yields or unwanted products on nitric acid oxidation, the indirect procedure of alkaline hydrolysis to p-methylbenzyl alcohol followed by chromic oxide-acetone oxidation to p-toluic acid was employed.

The first step in the sequence of operations leading to the determination of the reaction-center isotopic abundances of the reaction products was also an oxidation to a benzoic acid. Benzyl and p-chlorobenzyl methyl ethers gave satisfactory yields of benzoic and p-chlorobenzoic acids on permanganate oxidation, but p-methylbenzyl methyl ether required a less direct technique, namely hydriodic acid cleavage followed by hydrolysis to p-methylbenzyl alcohol followed by chromic oxide-acetone oxidation to p-toluic acid.

At this point in the degradations, the carbon atoms at the original reaction centers were in the form of carboxyl groups. To convert these groups to carbon dioxide for mass spectrometric analysis, use was made of the Schmidt decarboxylation reaction. Low yields were obtained in the case of p-chlorobenzoic acid under normal Schmidt

conditions, and a modified version of the reaction was developed for this acid. Pursuant to this development, a number of electronegatively-substituted benzoic acids were successfully decarboxylated using the new method. A description of this work is given in Appendix C.

The carbon dioxide produced by the decarboxylation reaction was analyzed by means of an isotope-ratio, 15-inch Nier-type mass spectrometer, carbon dioxide from a product being compared to carbon dioxide from its starting material. After corrections were made for the presence of oxygen isotopes (see Appendix A), the Stevens-Attree relationship gave k^{12}/k^{13}, the kinetic isotope effect.

2. The α-Toluenesulphonyl Bromide-Bromide Ion Reaction

The mechanism of this reaction was under investigation by other workers in this department (Prof. J.F. King and Dr. D.J.H. Smith), and a determination of its carbon-13 kinetic isotope effect was carried out as a joint project with Dr. Smith.

Dr. Smith performed the preliminary work and supplied the author with pure samples of starting materials (in the form of the products of 100% reaction) and reaction products. All were benzyl bromides, and were oxidized directly to benzoic acids using alkaline permanganate.

Decarboxylations and isotopic analyses were done in exactly the same manner as was used in the work described above.

B. Preparation of Materials

1. Benzyl chlorides

The benzyl chlorides used were obtained from commercial sources, and were redistilled before use on a 17-inch platinum spinning-band column.

Benzyl chloride :	b.p. 67°/15mm., n_D^{25} 1.5367
p-Chlorobenzyl chloride:	b.p. 97.5°/15mm., n_D^{25} 1.5549
p-Methylbenzyl chloride:	b.p. 78°/14mm., n_D^{20} 1.5332

2. Benzyl alkyl ethers

These were prepared by refluxing the corresponding benzyl chloride with 1M sodium alkoxide in alcohol. All were distilled on the column described above.

Benzyl methyl ether:	b.p. 61.5°/15mm., n_D^{25} 1.5010
Benzyl ethyl ether:	b.p. 78°/18mm., n_D^{20} 1.4954
p-Chlorobenzyl methyl ether:	b.p. 94°/15mm., n_D^{20} 1.5210
p-Methylbenzyl methyl ether:	b.p. 76°/13mm., n_D^{25} 1.5017

C. Kinetics

Because of the low solubility of sodium chloride in

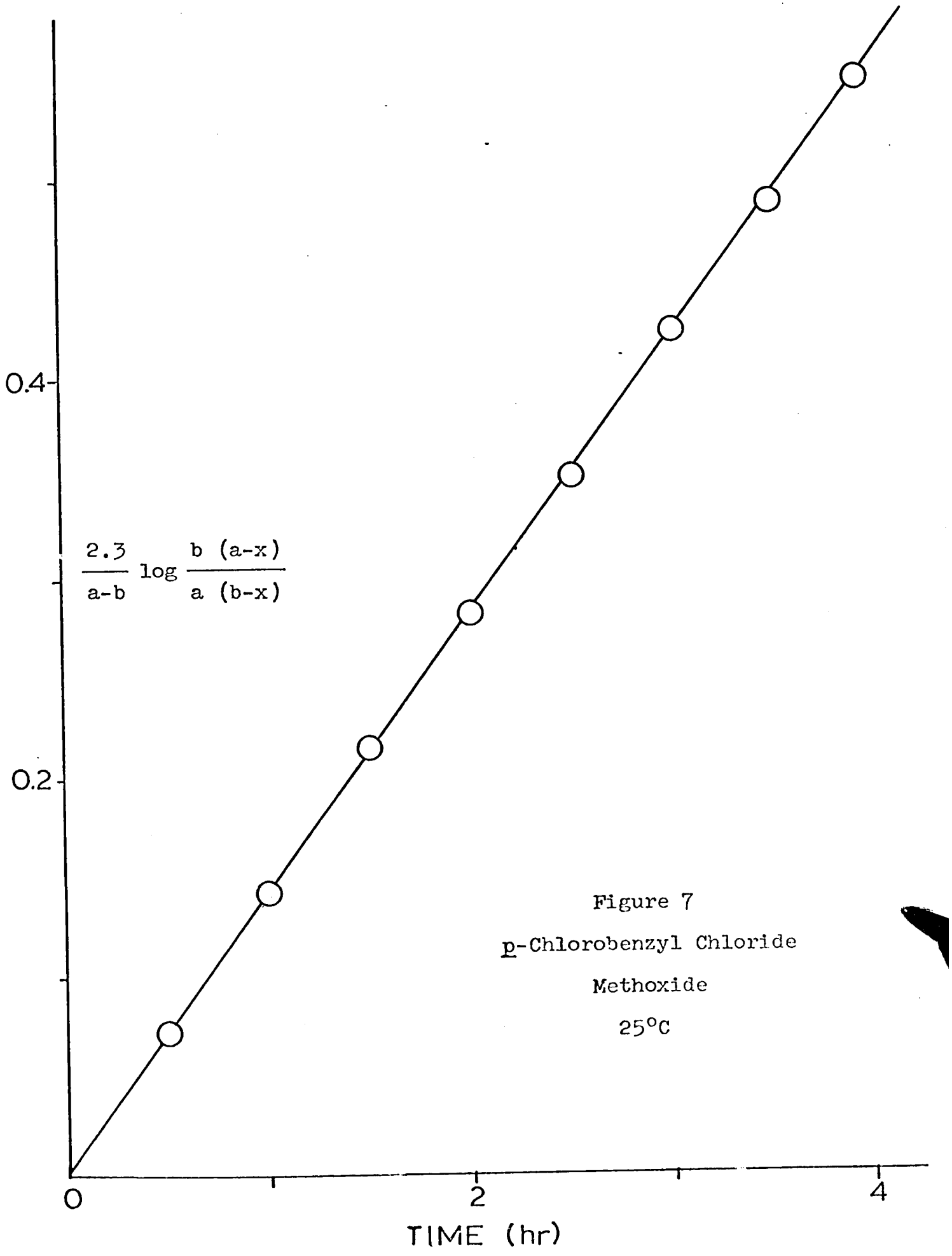

Figure 7

p-Chlorobenzyl Chloride

Methoxide

25°C

sodium methoxide-methanol solutions, it was not practical to use the common technique of analyzing aliquots taken at intervals from master runs. Instead, a number of separate samples of the reaction mixture was prepared and allowed to react simultaneously. Over a period of time, each in succession was quenched and analyzed. Quenching was accomplished by washing the entire sample into cold dilute nitric acid. Excess A.R. sodium bicarbonate was then added, and the chloride ion concentration determined by titration with silver nitrate in the presence of dichlorofluorescein.

The rate data so obtained are summarized in Table I and the results of a typical kinetic run are shown in Figure 7.

TABLE I

Kinetics of Benzyl Chloride Reaction with Sodium Alkoxide

Substituent	Alkoxide	Temperature	$10^5 k_2$ l-mole^{-1}min^{-1}
H	NaOEt	0	12.4
		25	219
	NaOMe	0	9.70
		25	168
p-Cl		0	7.42
		25	232
p-Me		0	16.0
		25	279
H	MeOH	25	3.68×10^{-6} min^{-1}

D. Isotope Effect Runs

After equilibration at the reaction temperature, the benzyl chloride (0.5 mole) was dissolved in a solution of sodium methoxide in methanol and allowed to react until 10 of the benzyl chloride had been consumed, at which time the reaction was quenched by pouring the mixture into an excess of 0.5 N nitric acid. This mixture was extracted with ether, and the extract, after drying over anhydrous magnesium sulphate, was carefully stripped of solvent.

E. Isolation of Reaction Product

1. Benzyl chloride series

Preparative gas-liquid chromatography on Apiezon N (15% on Chromosorb P) was used to separate both benzyl ethyl ether and benzyl methyl ether from unreacted benzyl chloride. The tendency of benzyl chloride to decompose on hot metal surfaced necessitated modification of a Nestor-Faust Prepko I unit, a glass column and preheater unit taking the place of the standard metal ones.

2. p-Chlorobenzyl chloride series

The p-chlorobenzyl methyl ether p-chlorobenzyl chloride reaction mixture was refluxed for six days with a solution of sodium carbonate (6 g.) in water (250 ml.). The cold

hydrolysis mixture was extracted with two 50 ml. portions of petroleum ether (b.p. 35-60°). After drying over magnesium sulphate, the combined extracts were evaporated to a volume of 30 ml. and cooled in ice. p-Chlorobenzyl alcohol crystallized and was removed by filtration. Further evaporation (to 15 ml.) followed by cooling in ice afforded more of the alcohol. The filtrate was then diluted to 50 ml. with fresh petroleum ether, and final traces of alcohol removed by treatment with Woelm alumina (Grade I).

3. p-Methylbenzyl chloride series

The p-methylbenzyl methyl ether-p-methylbenzyl chloride reaction mixture was distilled on a 17-inch platinum spinning band column. The fraction, b.p. 75-80°/13mm., was refluxed for three days with a solution of sodium carbonate (10 g.) in water (100 ml.). The cooled mixture was extracted with two 50 ml. portions of petroleum ether (b.p. 35-60°). The combined extracts, after drying over anhydrous magnesium sulphate, were treated with Woelm alumina (Grade I) to remove any p-methylbenzyl alcohol present.

F. Oxidations

1. Starting materials

a. Benzyl and p-Chlorobenzyl Chlorides

Benzyl (or p-chlorobenzyl) chloride (0.01 mole) was dissolved in pyridine (20 ml.). Water (40 ml.), potassium hydroxide (2 g.) and potassium permanganate (4 g.) were added, and the mixture heated, with stirring, for two hours. The cooled reaction mixture was poured into an ice-water mixture and acidified with hydrochloric acid. After the addition of sodium bisulphite to remove manganese dioxide, the mixture was extracted with ether. The extract was evaporated to dryness on a water-bath, and the residue recrystallized from water or ethanol-water. Yields of recrystallized acid were 88-92%.

b. p-Methylbenzyl chloride

A mixture of p-methylbenzyl chloride (3 g.), sodium carbonate (20 g.) and water (250 ml.) was refluxed for seventy-two hours. The mixture was then cooled in ice, and p-methylbenzyl alcohol filtered off. Recrystallization from petroleum ether gave 2.3 g. (88.5%) of p-methylbenzyl alcohol.

To a solution of this alcohol (1.0g.) in anhydrous acetone (50 ml.) was added, dropwise, a solution of chromic oxide (4.5 g.) in acetone (10 ml.) until the orange colour persisted for one minute. The reaction mixture was then poured into water (100 ml.) and the solid filtered off.

Recrystallization from ethanol-water gave 985 mg. (88%) of p-toluic acid,

2. Products

a. Benzyl and p-chlorobenzyl methyl ethers

These products were oxidized with alkaline potassium permanganate in pyridine-water in the same manner as that used to oxidize the parent benzyl chlorides. Trial runs using the pure ethers showed the yields under these conditions to be in the range of 90-95%.

b. p-Methylbenzyl methyl ether

This product was refluxed with 57 hydriodic acid (4 ml.) for 2.5 hours, and the cooled mixture then poured into a solution of sodium carbonate (20 g.) in water (250 ml.). This mixture was refluxed for 14 hours, cooled, and extracted with ether. The extract, after drying over anhydrous magnesium sulphate, was stripped of ether, and dissolved in anhydrous acetone (50 ml.). A solution of chromic oxide (4 g.) in acetone (10 ml.) was added dropwise until the orange colour persisted for one minute. The solution was then poured into water (250 ml.) and extracted with ether. The extract was evaporated to dryness on a water-bath, and the residue recrystallized from ethanol-water.

Trial runs using pure p-methylbenzyl methyl ether gave overall yields of p-toluic acid above 70%.

3. Nitric acid oxidation of p-methylbenzyl chloride

p-Methylbenzyl chloride (609 mg.) was refluxed with nitric acid (6 ml.) and water (21 ml.) for six days. After dilution with water, the reaction mixture was filtered. The white solid (496 mg.) was recrystallized from ethanol-water.

The product, m.p. 200-1°, was not p-toluic acid (lit. m.p. 178-9°). Its neutralization equivalent was 170. Sodium fusion showed the presence of chlorine and the absence of nitrogen. Schmidt degradation followed by acetylation gave an acetanilide m.p. 105°. The N.M.R. spectrum of the acetanilide indicated the presence of two methyl groups and three aromatic protons. It is thus either 2'- or 3'-chloro-p-acetotoluidide. The literature m.p. (38) of the 3' isomer is 105°.

Hydrolysis and chromic-oxide-acetone oxidation of a sample of the same starting material gave p-toluic acid.

G. Decarboxylation of the Benzoic Acids

The reaction train used was made up of a reactor with interchangeable flasks, and two gas scrubbers, the second being an alkali trap. A 5% solution of potassium permanganate

in 2N sulphuric acid was used in the first scrubber to prevent the carry-over of sulphur dioxide should any be formed in the reactor. The alkali trap was charged with 50 ml. of 0.2N sodium hydroxide solution freshly prepared from stock 1N carbonate-free alkali (made from sodium by the method of Calvin et.al. (39)).

With an empty reaction tube in place, the train was flushed with carbon dioxide-free nitrogen.

Approximately one millimole of the benzoic acid was weighed into a second reaction tube and dissolved, with heating, in 5 ml. of sulphuric acid. (96% acid for benzoic and p-toluic acids, 100% acid for p-chlorobenzoic acid.) The tube and its contents were then chilled in ice-water. Approximately 1.2 millimole of sodium azide was added to the contents of the tube, which was then quickly attached to the reaction-absorption train. An oil bath maintained at 40° was placed around the reaction flask, and the reaction allowed to proceed for two hours.

The contents of the trap were washed into a 125 ml. Erlenmeyer flask. 10 ml. of 1M ammonium chloride and 20 ml. of 1M barium chloride were added, the flask stoppered and shaken, and the mixture allowed to stand for at least two hours.

The precipitate was filtered on a medium-porosity sintered-glass filter, washed repeatedly with boiling water, and dried at 110°.

Trial runs on the pure acids (see Appendix C) showed yields to be greater than 90%.

H. Preparation of carbon dioxide samples for mass spectrometric analysis

Carbon dioxide was liberated from the barium carbonate from the Schmidt decarboxylations by means of concentrated sulphuric acid using standard high-vacuum techniques.

CHAPTER III

RESULTS

The carbon-13 kinetic isotope effects, k^{12}/k^{13}, found for the benzyl chloride-alkoxide ion systems studied here are shown in Tables II - VI.

The errors shown are mean deviations.

TABLE II

Reaction of Benzyl Chloride with Methoxide Ion in Methanol

Temp.	Run	k^{12}/k^{13}
25°	1E12 1E13 1E14 Average	1.0470 1.0462 1.0461 1.0464 ±0.0004
0°	1F20 1F21 1F22 Average	1.0503 1.0506 1.0491 1.0500 ±0.0006

TABLE III

Reaction of Benzyl Chloride with Ethoxide Ion in Ethanol

Temp.	Run	k^{12}/k^{13}
25°	1G1 1G2 1G3 Average	1.0482 1.0476 1.0473 1.0477 ±0.0003
0°	1H8 1H9 1H10 Average	1.0497 1.0514 1.0503 1.0503 ±0.0006

TABLE IV

Reaction of p-Chlorobenzyl Chloride with Methoxide Ion in Methanol

Temp.	Run	k^{12}/k^{13}
25°	5E1 5E2 5E3 Average	1.0493 1.0494 1.0495 1.0494 ±0.0001
0°	5F1 5F2 5F3 Average	1.0533 1.0534 1.0520 1.0529 ±0.0006

TABLE V

Reaction of p-Methylbenzyl Chloride with Methoxide Ion in Methanol

Temp.	Run	k^{12}/k^{13}
25°	4E4	1.0429
	4E5	1.0410
	4E6	1.0423
	Average	1.0421 ±0.0007
0°	4F4	1.0472
	4F5	1.0461
	4F6	1.0485
	Average	1.0473 ±0.0007

TABLE VI

Methanolysis of Benzyl Chloride at 25°C

Run	k^{12}/k^{13}
1A1	1.0361
1A3	1.0364
1A4	1.0364
Average	1.0363 ±0.0001

CHAPTER IV

DISCUSSION OF RESULTS

In a 'simple' nucleophilic substitution reaction,

$$Y^- + RX \longrightarrow YR + X^-$$

the attacking group, Y^-, 'pushes off' the leaving group, X^-. Formation of the new Y-R bond and rupture of the original R-X bond occur simultaneously.

The system moves along a reaction coordinate between the stable reactants and products, each of which represents a potential-energy minimum on the coordinate. This is illustrated in Figure 8.

The most significant feature of Figure 8 is the maximum in the curve, for it is the difference between the energy of the system at this point and the energy of the reactants which determines the rate of the reaction.

Since bond formation and rupture are synchronous, it is only natural to picture a continuous series of transitory 'structures', each with its C-Y bond partly formed and

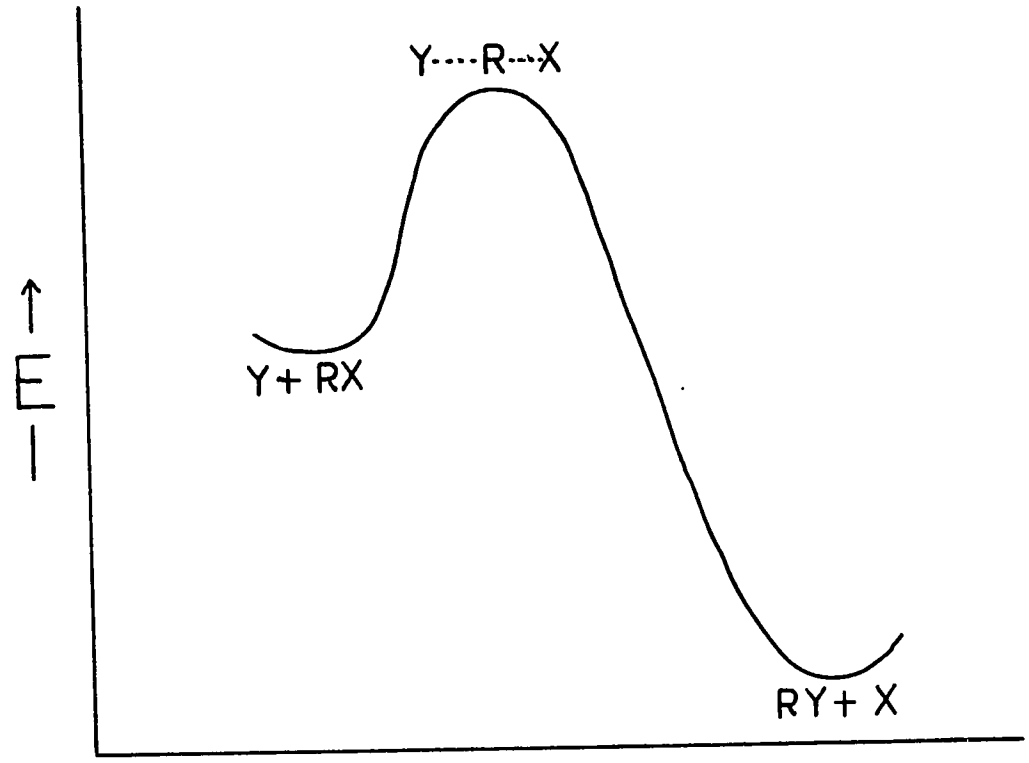

Figure 8

its C-X bond partly broken, corresponding to all the points constituting the curve in Figure 8.

The simple stratagem of considering one particular such 'structure' as if it were a chemical entity has been generally adopted and has proven to be useful in the study of reaction kinetics and mechanisms, although this species differs from a normal compound in that one degree of freedom is lost.

That 'structure,' as one might expect, is the one corresponding to the potential energy maximum on the path

between reactants and products. It has been variously named as the activated complex and the transition state.

Compared to real structures, the transition state lacks a degree of freedom along the reaction coordinate; with this important difference in mind, the transition state can usually be discussed usefully in terms of the behavior of stable species.

Direct evidence for the 'structure' of the transition state is unobtainable, and a variety of approaches, both theoretical and experimental, has been devised to probe its nature by means of indirect measurements.

In principle, it is possible to use the theory of absolute reaction rates (20) to compute the rate for any given transition state model, and thus to arrive at the true 'structure' by a comparison of the observed reaction rate with those calculated for a variety of reasonable models. In practice, however, except for the simplest of gas-phase reactions, such an endeavour demands a far more precise knowledge of the physical parameters involved than is realizable. This is especially true for reactions in the condensed phase, where the complex effects of solvation must also be accounted for.

Many of the factors which are difficult to estimate

with a useful degree of precision can be eliminated by cancellation through a study of comparative rates for a closely related series of compounds. The study of the relative reaction rates of variously substituted reactants is a popular version of this approach, and may be valid to a high degree of approximation provided that the substituents are sufficiently remote from the reaction site that their effect on the reaction mechanism is due to but a single factor such as, for example, their polarity. In practice, however, this method has shown itself to be capable of yielding only qualitative, or at best, semi-quantitative answers to the question of transition state structure.

Isotopic substitution at the reaction center constitutes a more subtle means of eliminating, by cancellation, some of the unknowns, for in this case only the mass of a single nucleus is changed; the nuclear positions are but slightly altered, and the electron distributions are generally assumed to be unaffected. Relative rate studies on such isotopically substituted reactants, i.e. kinetic isotope effect studies, would thus appear to offer a potentially powerful tool for the investigation of transition states.

The very subtlety of the changes so induced, however,

creates a new problem, for the rate changes so produced are intimately related to the vibrational modes in the transition state and in the reactants, with the result that a detailed theoretical analysis may be required to elicit useful conclusions. It is significant, however, that in many cases successful analyses have been made on the basis of very simple models.

Primary deuterium kinetic isotope effect studies yield qualitative details about transition state structure without requiring recourse to any rigorous theoretical analysis; Melander (40) and Westheimer (21) have, independently, presented theoretical arguments to show that one can decide whether a given transition state is reactant-like or product-like in processes involving linear three-center proton transfers. The limiting requirement for this analysis is that the mass of the central atom of the three-center transition state be very small compared to the masses of the other two atoms involved. This method, therefore, may not be applicable to the interpretation of carbon isotope effects.

The most generally accepted theoretical treatment of kinetic isotope effects is that due to Bigeleisen. A detailed derivation of the Bigeleisen equations is given in Appendix B of this thesis. In the present discussion,

Equation 1 below, the so-called 'gamma-bar approximation' will be used throughout. The principal reason for this choice is that this particular expression employs variables which are such as to allow ready visualization of the relationship between the theoretical calculations and the physical models selected.

$$\frac{k_1 S_2 S_1^{\ddagger}}{k_2 S_1 S_2^{\ddagger}} = \frac{\nu_{1_L}^{\ddagger}}{\nu_{2_L}^{\ddagger}} \left[1 + \frac{\overline{\gamma}}{24} \left| \frac{\hbar c}{\kappa T} \right|^2 \sum_{j}^{3n} \left[\frac{1}{m_{1_j}} - \frac{1}{m_{2_j}} \right] \left[a_{jj} - a_{jj}^{\ddagger} \right] \right] \quad (1)$$

in which

k_1/k_2 = kinetic isotope effect

S = symmetry number

$\nu_{1_L}^{\ddagger}/\nu_{2_L}^{\ddagger}$ = temperature independent factor

$\hbar$ = Planck constant/2π

c = velocity of light

κ = Boltzman constant

T = absolute temperature

m = mass of isotopic atom

a_{jj} = bond stretching force constant

$\ddagger$ designates transition state

$1,2$ subscripts designating lighter and heavier isotopes respectively

The constant, $\overline{\gamma}$, from which Equation 1 derives its name, is defined by Equation 2:

$$\overline{\gamma} = \frac{12G(u)}{u} \qquad (2)$$

in which

$$G(u) = 1/2 - \frac{1}{u} + \frac{1}{e^{u} - 1}$$

and

$$u = \frac{hc\nu}{\kappa T}$$

The major work described in this thesis concerns the reaction between an alkoxide ion and a benzyl chloride.

Rate measurements showed these reactions to be strictly second-order kinetically, first-order in each reactant. By the usual definitions, all are clearly bimolecular substitution reactions.

For the theoretical calculations of the carbon-13 kinetic isotope effects in the alkoxide-benzyl chloride reactions, the simple linear transition state model shown in Figure 9 was used.

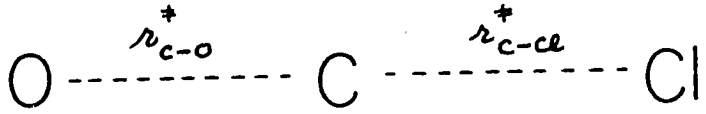

Figure 9

It was assumed that the only bond in the reactants that is altered on passing along the reaction coordinate is the carbon-chlorine bond.

The temperature-independent factor, $\nu_{1_L}^{\ddagger}/\nu_{2_L}^{\ddagger}$ was calculated by means of Equation 3, the Bigeleisen three-center reaction coordinate for the reaction

$$X + YZ \longrightarrow XY + Z$$

$$\frac{\nu_{1_L}^{\ddagger}}{\nu_{2_L}^{\ddagger}} = \left[\frac{\frac{1}{m_{Y(1)}} + \frac{1}{m_{Z(1)}} + \frac{\beta^2}{\alpha^2}\left[\frac{1}{m_{Y(1)}} + \frac{1}{m_{X(1)}}\right] + 2\frac{\beta}{\alpha}\frac{1}{m_{Y(1)}}}{\frac{1}{m_{Y(2)}} + \frac{1}{m_{Z(2)}} + \frac{\beta^2}{\alpha^2}\left[\frac{1}{m_{Y(2)}} + \frac{1}{m_{X(2)}}\right] + 2\frac{\beta}{\alpha}\frac{1}{m_{Y(2)}}} \right]^{1/2} \quad (3)$$

For Model 1 shown in Figure 9, and using the Slater theorem in regard to the choice of m's, Equation 3 becomes Equation 4.

$$\frac{\nu_{1_L}^{\ddagger}}{\nu_{2_L}^{\ddagger}} = \left[\frac{\frac{1}{12} + \frac{1}{35} + \frac{\beta^2}{\alpha^2}\left[\frac{1}{12} + \frac{1}{16}\right] + 2\frac{\beta}{\alpha}\frac{1}{12}}{\frac{1}{13} + \frac{1}{35} + \frac{\beta^2}{\alpha^2}\left[\frac{1}{13} + \frac{1}{16}\right] + 2\frac{\beta}{\alpha}\frac{1}{13}} \right]^{1/2} \quad (4)$$

The term β/α in Equations 3 and 4 is the ratio of 'bond formation' to 'bond rupture' in the transition

state 'stretching force constants' for the two 'bonds' in Figure 9.

$$\frac{\beta}{\alpha} = \frac{(a_{jj}^{\ddagger})_{c-o}}{(a_{jj}^{\ddagger})_{c-cl}} \qquad (5)$$

The temperature-independent factor thus defined for Model 1 is plotted as a function of β/α in Figure 10.

A stretching frequency of 700 cm. was used in calculating the value of γ, the value so obtained being 0.850. The selection of a frequency in this regard is far from critical, a frequency of 1000 cm. , for example, leading to the only slightly higher value of 0.858 for γ. Indeed, it is this very lack of sensitivity to frequency in γ that is largely responsible for the utility of Equation 1; it is only necessary to have some idea of the magnitude of the 'u's which made the major contribution.

The simplifying assumption made earlier in regard to neglecting all bonds not directly involved in the reaction allows the summation term of Equation 1 to be rewritten:

$$\sum_{j}^{3n} \left[\frac{1}{m_{1_j}} - \frac{1}{m_{2_j}}\right]\left[a_{jj} - a_{jj}^{\ddagger}\right] = \left[\frac{1}{12} - \frac{1}{13}\right]\left[a_{c-cl} - a_{c-cl}^{\ddagger} - a_{c-o}^{\ddagger}\right] \qquad (6)$$

An empirical rule developed by Badger (41) relating bond lengths to stretching force constants was used to

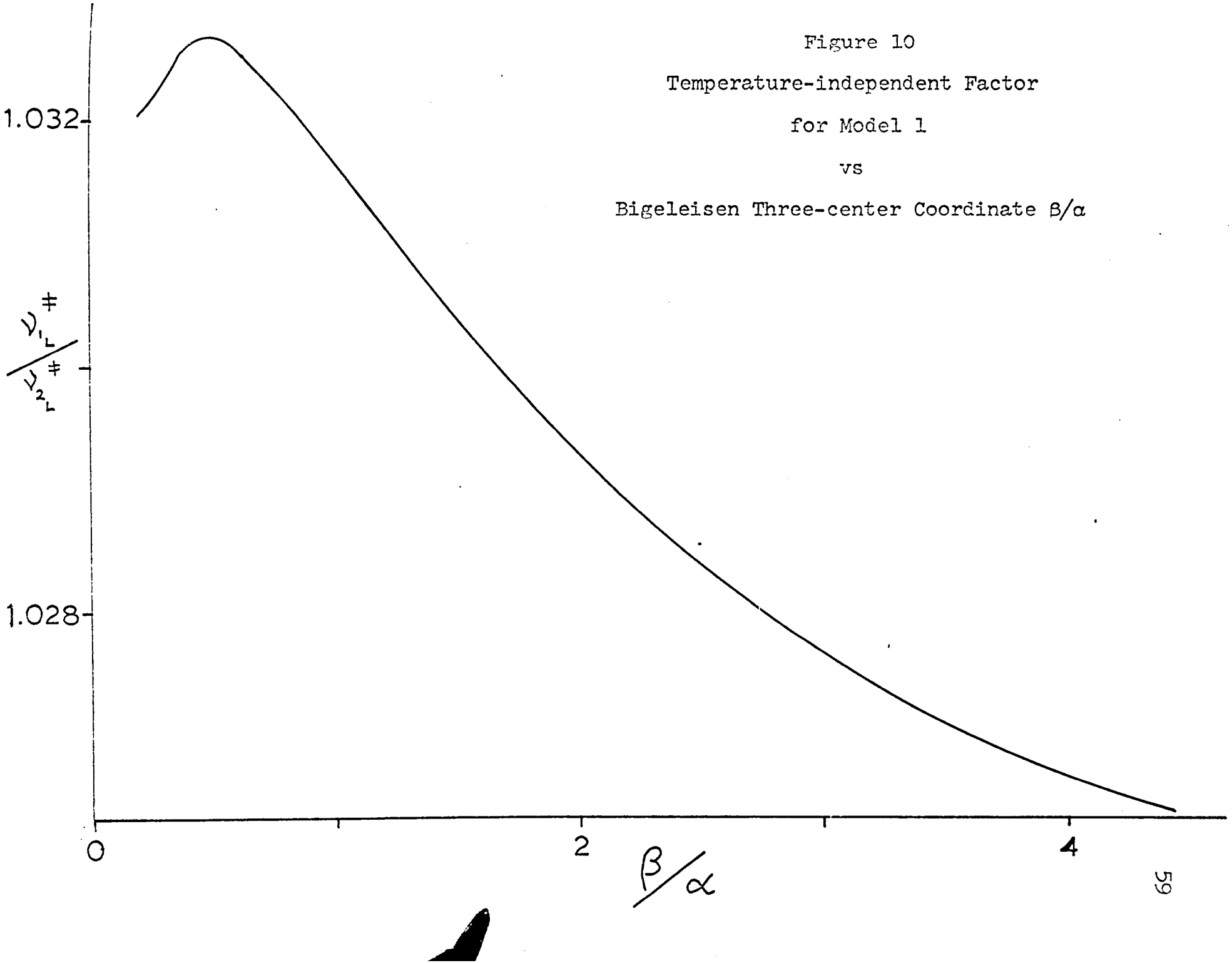

Figure 10

Temperature-independent Factor

for Model 1

vs

Bigeleisen Three-center Coordinate β/α

estimate 'stretching force constants' for the transition state carbon-chlorine and carbon-oxygen 'bonds'. Equation 7 is a statement of Badger's 'rule'.

$$r^{\ddagger} = \left[\frac{A}{a^{\ddagger}_{jj}}\right]^{1/3} + B \qquad (7)$$

in which

$r^{\ddagger}$ = 'bond length'

$a^{\ddagger}_{jj}$ = 'stretching force constant'

A,B = constants dependent on the rows of the periodic table in which the atoms forming the bond occur

The 'stretching force constants' calculated in this way are plotted against carbon-chlorine and carbon-oxygen 'bond lengths' in Figures 11 and 12.

Using the gamma-bar approximation, kinetic isotope effects, k^{12}/k^{13}, were calculated for Model 1 and a series of selected β/α values. Plots of these k^{12}/k^{13} values against β/α and carbon-chlorine bond extensions are shown in Figure 13.

If it is assumed for the benzyl chloride-methoxide ion reaction that the transition state is symmetrical, i.e. $\beta/\alpha = 1$, and that the carbon-chlorine 'bond' is 35% longer

Figure 11

'Stretching Force Constants'

vs

'Bond Elongation'

for

Carbon-Chlorine 'Bond'

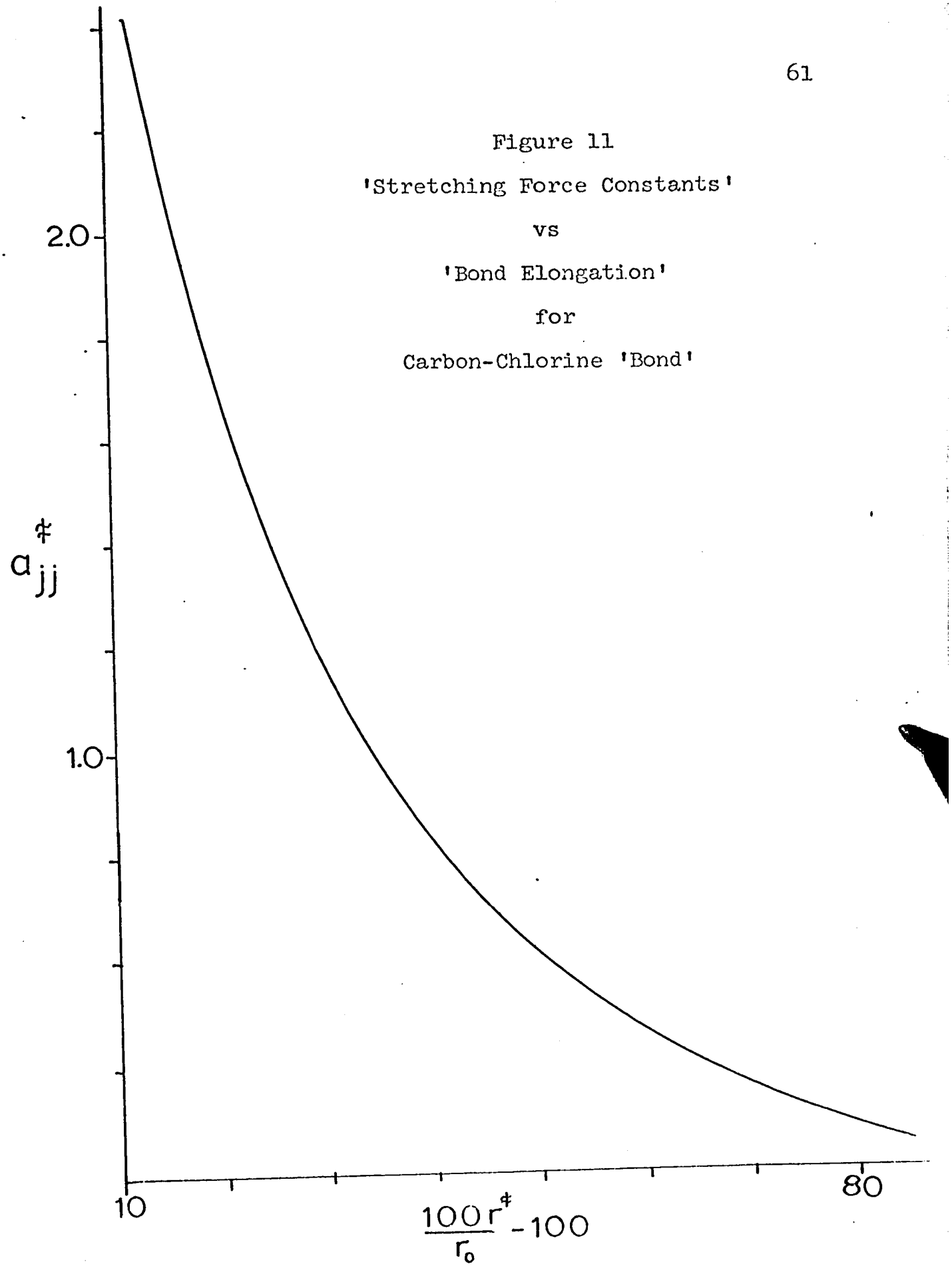

Figure 12

'Stretching Force Constants'

vs

'Bond Elongation'

for

Carbon-Oxygen 'Bond'

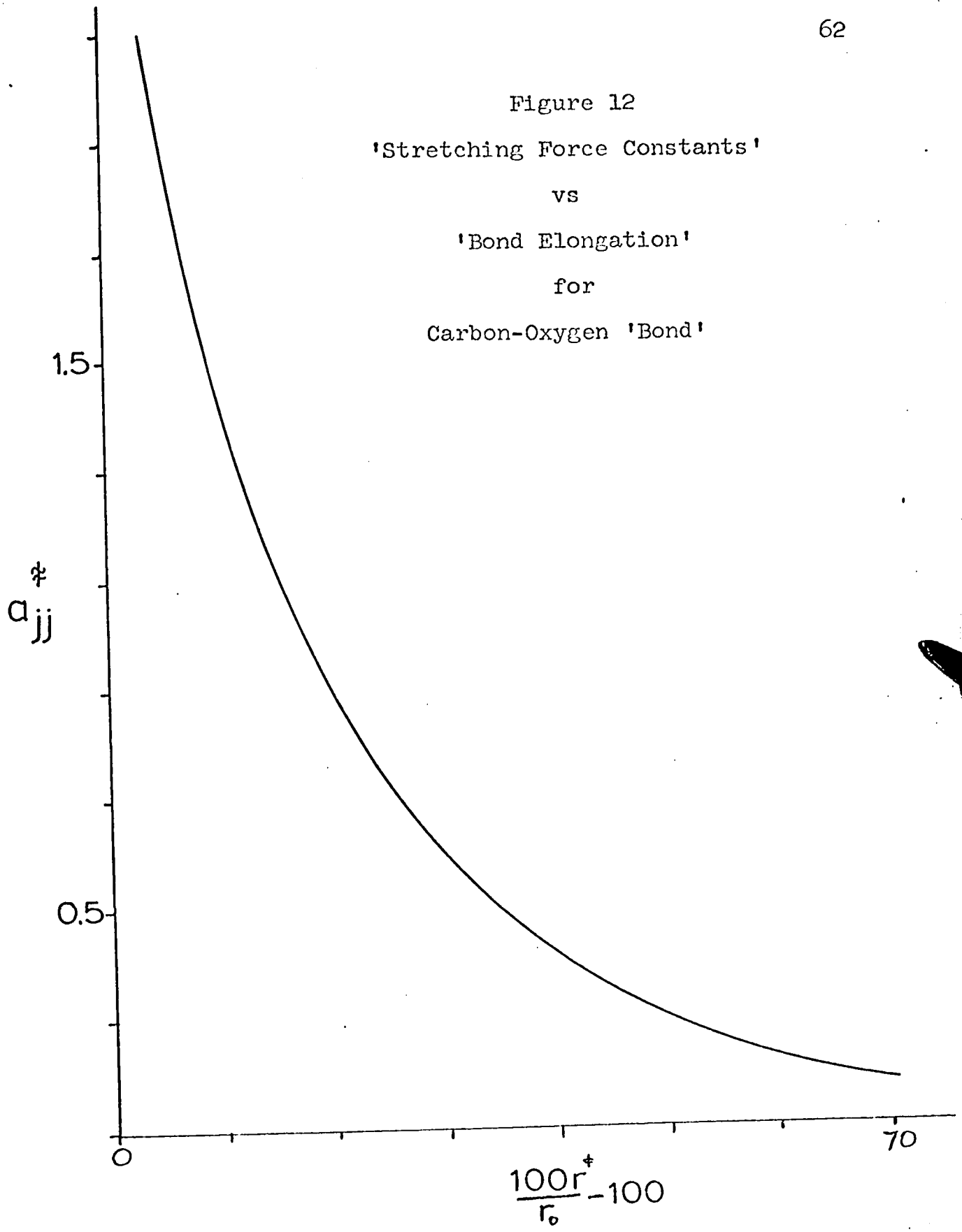

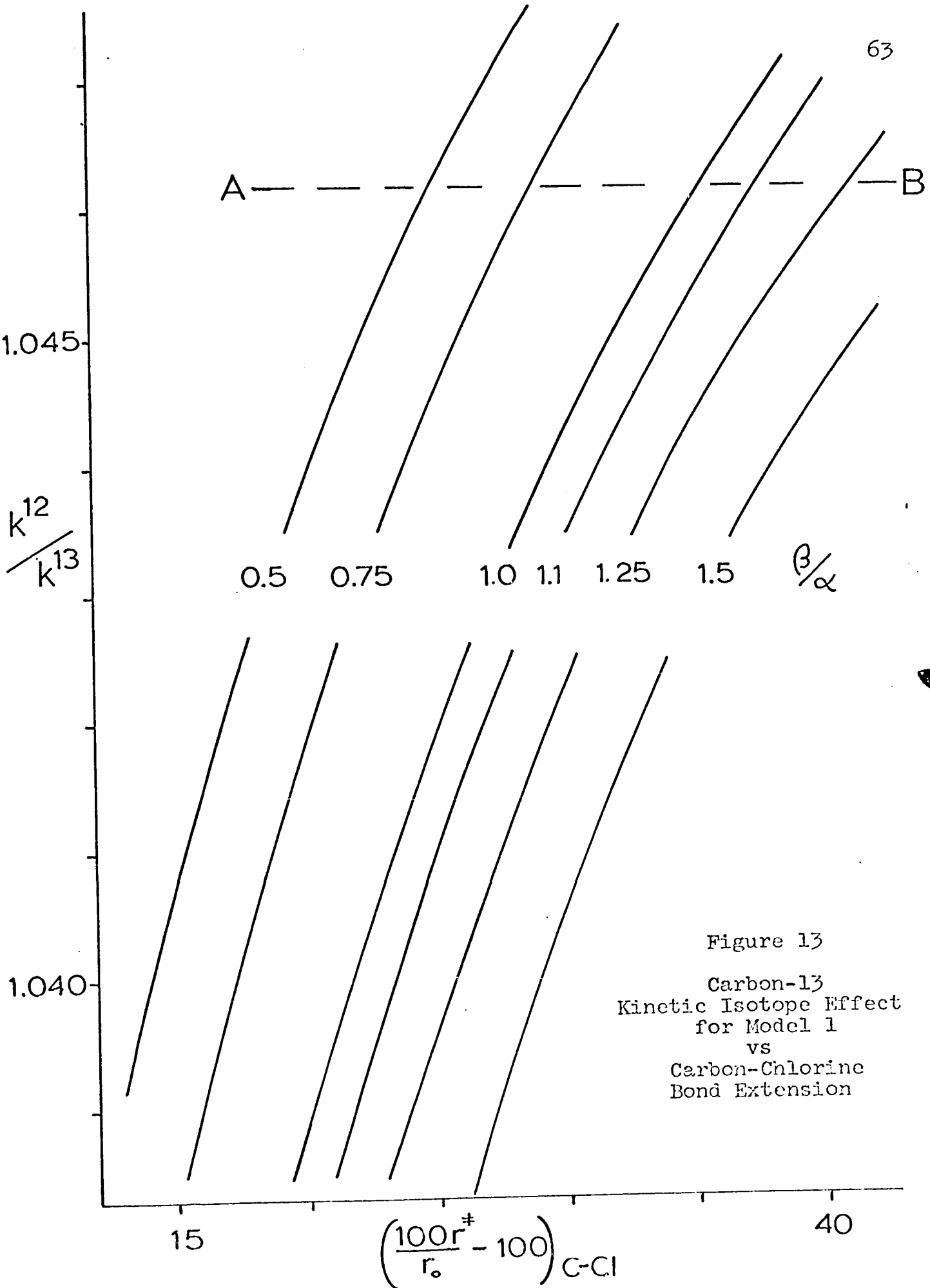

Figure 13

Carbon-13
Kinetic Isotope Effect
for Model 1
vs
Carbon-Chlorine
Bond Extension

than the carbon-chlorine bond of benzyl chloride, the calculated kinetic isotope effect for carbon-13 is 1.0462 at 25°C, and 1.0490 at 0°C. The experimental values are 1.0464 ± 0.0004 at 25°C and 1.0500 ± 0.0006 at 0°C.

While the excellence of this agreement between calculated and observed values may well be somewhat fortuitous, it nevertheless appears to validate the use of the Badger relationship in estimating transition state 'stretching force constants'.

It should be noted, however, that the value assumed by k^{12}/k^{13} based on a model in which only a 25% extension of the carbon-chlorine bond has occurred is also 1.0462 at 25° if a β/α value of 0.5 is used. In fact, a series of transition state models can be envisaged, each member of which corresponds to a point on the line AB in Figure 13, i.e. the $k^{12}/k^{13} = 1.0462$ line.

In short, the situation is this: for a given transition state geometry the gamma-bar approximation gives but one calculated k^{12}/k^{13} value; on the other hand, a given k^{12}/k^{13} value can be rationalized by a whole series of geometries.

It seems clear, therefore, that the transition state

geometry for a substitution reaction cannot be determined from a knowledge of the kinetic isotope effect alone. Some further criterion is needed.

It was hoped, at the beginning of the present work, that a study of the effect of substituents on the carbon-13 kinetic isotope effect would supply that criterion for the benzyl chloride-methoxide ion system.

To this end, kinetic isotope effect measurements were carried out on the reactions of methoxide ion with benzyl, p-chlorobenzyl and p-methylbenzyl chlorides. The results of that investigation are summarized in Table VII.

TABLE VII

The Carbon-13 Kinetic Isotope Effect
for the
Benzyl Chloride-Methoxide-ion Reaction

Substituent on Benzyl Chloride	k^{12}/k^{13} 25°C	k^{12}/k^{13} 0°C
p-Methyl	1.0421 ±0.0007	1.0473 ±0.0007
None	1.0464 ±0.0004	1.0500 ±0.0006
p-Chloro	1.0494 ±0.0001	1.0529 ±0.0006

In addition, Bukta (42) observed a carbon-13 kinetic isotope effect of 1.046 ± 0.007 for the reaction of m-bromobenzyl chloride with methoxide ion at 25°C.

Since the substituent effect shown by the tabulated data above is of an order of magnitude greater than the mean deviations of the observations, the effect is indeed real. A clear trend emerges, electron-donating substituents decreasing and electron-withdrawing substituents increasing the kinetic isotope effect. (The mean deviation of Bukta's figure for m-bromobenzyl chloride-methoxide is too large to permit any conclusions in this regard.)

It is interesting to consider here the tendencies predicted by the Swain-Thornton rule (34) with regard to the effect of changes in electron density at the central carbon atom of a three-center transition state.

The rule predicts that electron-donating substituents on the central atom will lengthen both the carbon-chlorine and carbon-oxygen 'bonds' in the transition state for the system being considered here, and that electron-withdrawing substituents will have the opposite effect on these 'bonds'.

Thornton's revised statement (36) of this rule leads to the same predictions.

Since a longer transition state 'bond' involves a

smaller 'stretching force constant', the Swain-Thornton rule, in conjunction with the gamma-bar approximation of Bigeleisen (see Appendix B), predicts a higher kinetic isotope effect for p-methylbenzyl chloride-methoxide than for benzyl chloride-methoxide, and a smaller one for p-chlorobenzyl chloride-methoxide.

This prediction is in striking contrast with the experimental results reported here.

Intuitively one would certainly expect that an increased electron supply at the benzylic position would lengthen the carbon-chlorine transition state 'bond'. If one accepts that such is the case, then, in terms of the model used (Model 1, Figure 9), a concomittant carbon-oxygen 'bond' shortening must take place.

One model which will fit the observed 25° kinetic isotope effect for the benzyl chloride reaction with methoxide ion is one in which the carbon-chlorine bond has been extended by 30% with $\beta/\alpha = 0.75$. If the carbon-chlorine 'bond' is longer than this in the transition state for the p-methylbenzyl chloride-methoxide ion reaction, say 35% extended, β/α must be 1.50 in order that the calculated effect equal the observed value; this involves a shortening of the carbon-oxygen 'bond' from 63% 'extended' to only 45% 'extended'.

It is no more reasonable, however, to expect a carbon-oxygen 'bond' shortening under these circumstances than to expect a carbon-chlorine 'bond' shortening; intuition and the Swain-Thornton rule are in agreement on that point. Both bonds must lengthen.

Obviously, then, Model 1 is inadequate in some way. It appears to be good enough to give predictions in reasonable agreement with any single observed value, but is deficient when it comes to handling small changes in structure.

In terms of the Swain-Thornton 'starred-wavemarked' diagram for the benzyl chloride-methoxide ion transition state, the carbon-carbon bond between the ring and the α-position is wavemarked. Accordingly, it should undergo shortening in the transition-state with increased electron supply.

In terms of resonance theory, it is highly probable that the plane of the aromatic ring is perpendicular to the axis of the bonds undergoing change in the reaction and that the electron clouds associated with those bonds is parallel to the axis of the π-bonds of the ring; the situation is ideally suited for overlap and therefore for resonance transmission of the substituent effect to the benzylic position, i.e. the reaction site. In effect,

then, the ring-α-carbon bond achieves a bond order fractionally greater than one, i.e. assumes partial double bond character and thus shortens.

It seems reasonable to expect that this ring-α-carbon length-change would change in a regular fashion in the series p-methyl, p-hydrogen, p-chloro in such a way as to be greatest for the p-methyl case.

If this situation obtains, the summation term in Equation 1 becomes

$$\sum_{j}^{3n} \left[a_{jj} - a_{jj}^{\ddagger} \right] = \underset{c\text{-}Cl}{\Delta a_{jj}} + \underset{c\text{-}C}{\Delta a_{jj}} + \underset{c\text{-}O}{\Delta a_{jj}} \qquad (8)$$

In this regard, it should be noted that, for a model based on a 35% carbon-chlorine extension and a β/α value of 1, shortening the ring-α-carbon bond by only 1% completely negates the effect on the isotope effect of an increase of 10% in both the other bond extensions.

The benzyl chloride-alkoxide ion system was chosen for the present investigation primarily because it offered a combination of a clean-cut well-understood S_N2 reaction and a means of physically separating the substituent from the reaction center and thus a means of avoiding the complication of steric effects. Unfortunately, it suffers

from the drawback of introducing a different complication, i.e. resonance interaction with the reaction site.

At present it is not possible to assess the extent of such interaction in a quantitative way. As a result, for this system at least, substituent effects cannot provide the necessary additional information needed for a choice between the various transition state geometries which the gamma-bar approximation offers.

The Benzyl-Chloride-Ethoxide-ion Reaction

According to the Swain-Thornton rule, increasing the electron density in the attacking group leads to a lengthening of the transition state bond between that group and the reaction center, and a shortening of the bond between the reaction center and the leaving group. In the benzyl chloride-alkoxide ion transition state this corresponds to a greater carbon-oxygen bond length and a shorter carbon-chlorine one.

The stretching force constant for a carbon-oxygen bond is much larger than that for a carbon-chlorine bond. A given increase in the length of the former will therefore have a greater effect on the summation term in Equation 1 than the same change in the latter bond. It would therefore

be expected that increased electron density in the attacking group would lead to a higher kinetic isotope effect.

The present results indicate that such is the case, since the reaction of ethoxide ion with benzyl chloride exhibits a larger kinetic isotope effect than does the methoxide ion reaction.

	k^{12}/k^{13} 25°
OMe^-	1.0464 ±0.0004
OEt^-	1.0477 ±0.0003

The Methanolysis of Benzyl Chloride

Whether one considers the methanolysis of benzyl chloride to be S_N1-like, in which case resonance stabilization by the ring would lead to a smaller isotope effect, compared to that observed in the benzyl chloride-methoxide reaction, or whether one considers the reaction to be S_N2-like, in which case reduced electron density in the attacking group would also lead to a smaller isotope effect, the fact is that the observed isotope effect is smaller, being only 1.0363 ±0.0001 at 25°.

No mechanistic conclusions can be drawn from this single piece of evidence.

APPENDIX A

MASS SPECTROMETRIC ANALYSES

The mass spectrometer employed for the isotopic abundance measurements is a dual-collection, ratio-recording instrument by which the mass 45 peak is compared to the combined 44 and 46 peaks. The readings must be corrected for the contributions of oxygen isotopes.

The value of the ratio r, where

$$r = \frac{(^{12}C/^{13}C)_{reactant}}{(^{12}C/^{13}C)_{product}} \qquad (1)$$

is required for the evaluation of k^{12}/k^{13}, the kinetic isotope effect, whereas the instrument reading, R, is

$$R = \frac{\left[K \frac{45}{44 + 46}\right]_1}{\left[K \frac{45}{44 + 46}\right]_2} = \frac{\left[\frac{45}{44 + 46}\right]_1}{\left[\frac{45}{44 + 46}\right]_2} \qquad (2)$$

where the subscript 1 refers to the carbon dioxide from the

reactant and subscript 2 refers to the carbon dioxide from the product. K is the machine constant whose value need not be determined.

For carbon dioxide,

$$\frac{45}{44+46} = \frac{[^{13}C^{16}O^{16}O]+[^{12}C^{16}O^{17}O]}{[^{12}C^{16}O^{16}O]+[^{12}C^{17}O^{17}O]+[^{12}C^{18}O^{16}O]+[^{13}C^{16}O^{17}O]} \quad (3)$$

$[^{12}C^{17}O^{17}O]$ and $[^{13}C^{16}O^{17}O]$ are negligible compared to $[^{12}C^{16}O^{16}O]$ and $[^{12}C^{16}O^{18}O]$, so that

$$\frac{45}{44+46} = \frac{[^{13}C^{16}O^{16}O]+[^{12}C^{16}O^{17}O]}{[^{12}C^{16}O^{16}O]+[^{12}C^{16}O^{18}O]} \quad (4)$$

Substitution of

$$[^{12}C^{16}O^{18}O] = 2\frac{^{18}O}{^{16}O}[^{12}C^{16}O^{16}O] \quad (5)$$

gives

$$\frac{45}{44+46} = \frac{[^{13}C^{16}O^{16}O]+[^{12}C^{16}O^{17}O]}{[^{12}C^{16}O^{16}O]+[\ 1+2^{18}O/^{16}O]} \quad (6)$$

Substitution of

$$\frac{[^{13}C^{16}O^{16}O]}{[^{12}C^{16}O^{16}O]} = \frac{^{13}C}{^{12}C} \tag{7}$$

and

$$\frac{[^{12}C^{16}O^{17}O]}{[^{12}C^{16}O^{16}O]} = 2\frac{^{17}O}{^{16}O} \tag{8}$$

gives

$$\frac{45}{44 + 46} = \left[\frac{^{13}C}{^{12}C} + 2\frac{^{17}O}{^{16}O}\right]\left[\frac{1}{1 + \frac{^{18}O}{^{17}O}}\right] \tag{9}$$

Equation 2 then becomes

$$R = \frac{\left[\frac{^{13}C}{^{12}C}\right]_1 + 2\frac{^{17}O}{^{16}O}}{\left[\frac{^{13}C}{^{12}C}\right]_2 + 2\frac{^{17}O}{^{16}O}} \tag{10}$$

Rearranged, Equation 10 becomes

$$\frac{\left[\frac{^{13}C}{^{12}C}\right]_1}{\left[\frac{^{13}C}{^{12}C}\right]_2} = R + \frac{2\left[\frac{^{17}O}{^{16}O}\right]\left(R-1\right)}{\left[\frac{^{13}C}{^{12}C}\right]_2} = \frac{1}{r} \qquad (11)$$

Letting $\left[\frac{^{17}O}{^{16}O}\right] = 0.00039$

and $\left[\frac{^{13}C}{^{12}C}\right] = \frac{0.011}{0.989}$

$$^1/r = \frac{\left[\frac{^{13}C}{^{12}C}\right]_1}{\left[\frac{^{13}C}{^{12}C}\right]_2} = R + 0.070(R-1) = \frac{\left[\frac{^{12}C}{^{13}C}\right]_2}{\left[\frac{^{12}C}{^{13}C}\right]_1} \qquad (12)$$

Equation 12 has been employed for all the determinations reported in this thesis.

APPENDIX B

THE BIGELEISEN EQUATIONS

The following derivation has been assembled from a number of sources (18,19,40,43,44,45,46), since the literature does not appear to provide a complete and orderly development of the Bigeleisen treatment of isotope effects.

For the parallel reactions

$$1 + B \xrightarrow{k_1} \text{products} \qquad (1)$$

and

$$2 + B \xrightarrow{k_2} \text{products} \qquad (2)$$

in which 1 and 2 represent isotopic species, transition state theory (20) gives these well-known equations for the rate constants:

$$k_1 = \frac{\kappa T}{h} x_1 K_1^{\neq} \qquad (3)$$

and

$$k_2 = \frac{\kappa T}{h} x_2 K_2^{\neq} \qquad (4)$$

in which

κ is the Boltzman constant

T is the absolute temperature

h is the Planck constant

x is the transmission coefficient

$K^{\ddagger}$ is the equilibrium constant for the quasi-equilibrium between the transition state and the reactants

In terms of partition functions, $K_1^{\ddagger}$ and $K_2^{\ddagger}$ are defined by Equations 5 and 6:

$$K_1^{\ddagger} = \frac{Q_1^{\ddagger}}{Q_1 Q} \tag{5}$$

$$K_2^{\ddagger} = \frac{Q_2^{\ddagger}}{Q_2 Q} \tag{6}$$

in which $Q_1^{\ddagger}$ and $Q_2^{\ddagger}$ are the complete functions of the transition states which lack the degree of freedom along the path of decomposition

and Q_1, Q_2 and Q are the complete partition functions of the reactants.

Thus it follows that

$$\frac{k_1}{k_2} = \frac{x_1 \; Q_2 \; Q_1^{\ddagger}}{x_2 \; Q_1 \; Q_2^{\ddagger}} \tag{7}$$

If it is assumed that the transmission coefficients, x_1 and x_2, are equal, Equation 7 becomes

$$\frac{k_1}{k_2} = \frac{Q_2 Q_1^{\ddagger}}{Q_1 Q_2^{\ddagger}} \tag{8}$$

The Term Q_2/Q_1

To a good approximation, the total partition coefficient, Q, is equal to the product of the individual partition functions Q_t (translational), Q_r (rotational), Q_v (vibrational) and Q_e (electronic):

$$Q = Q_t Q_r Q_v Q_e \tag{9}$$

For a non-linear molecule, the partition coefficient, Q, is thus

$$Q = \frac{(2\pi M \kappa T)^{3/2}}{h^3} V \cdot \frac{8\pi^2 (8\pi^3 I_A I_B I_C)^{1/2} (\kappa T)^{3/2}}{hs} \cdot$$

$$\prod_{i}^{3n-6} \frac{l^{\frac{-hc\nu_i}{2\kappa T}}}{1 - l^{\frac{-hc\nu_i}{\kappa T}}} \cdot 1 \tag{10}$$

and Q_2/Q_1 is therefore

$$\frac{Q_2}{Q_1} = \frac{S_1}{S_2}\left[\frac{M_2}{M_1}\right]^{3/2}\left[\frac{I_{A_2} I_{B_2} I_{C_2}}{I_{A_1} I_{B_1} I_{C_1}}\right]^{1/2}\prod_i^{3n-6} \ell^{\frac{hc}{2\kappa T}(\nu_{1i}-\nu_{2i})} \frac{1-\ell^{-\frac{hc\nu_{1i}}{\kappa T}}}{1-\ell^{-\frac{hc\nu_{2i}}{\kappa T}}} \tag{11}$$

The classical value of Q_2/Q_1 is

$$\frac{Q_2}{Q_1} = \prod_j^{n}\left[\frac{m_{2j}}{m_{1j}}\right]^{3/2} \tag{12}$$

Equation 11 approaches the classical value at high temperatures. Thus, since

$$\lim_{T\to\infty}\left[\ell^{\frac{hc}{\kappa T}(\nu_{1i}-\nu_{2i})}\right] = 1 \tag{13}$$

$$\lim_{T\to\infty}\left[\frac{1-\ell^{-\frac{hc\nu_{1i}}{\kappa T}}}{1-\ell^{-\frac{hc\nu_{2i}}{\kappa T}}}\right] = \frac{\nu_{1i}}{\nu_{2i}} \tag{14}$$

Equation 11 becomes, at high temperatures, Equation 15, i.e.

$$\left[\frac{I_{A_2} I_{B_2} I_{C_2}}{I_{A_1} I_{B_1} I_{C_1}}\right]^{1/2}\left[\frac{M_2}{M_1}\right]^{3/2}\prod_i^{3n-6}\frac{\nu_{1i}}{\nu_{2i}} = \prod_j^{n}\left[\frac{m_{2j}}{m_{1j}}\right]^{3/2} \tag{15}$$

or

$$\left[\frac{I_{A_2} I_{B_2} I_{C_2}}{I_{A_1} I_{B_1} I_{C_1}}\right]^{1/2} \left[\frac{M_2}{M_1}\right]^{3/2} = \prod_j^n \left[\frac{m_{2j}}{m_{1j}}\right]^{3/2} \prod_i^{3n-6} \left[\frac{\nu_{2i}}{\nu_{1i}}\right] \tag{16}$$

or

$$\prod_j^n \left[\frac{m_{1j}}{m_{2j}}\right]^{3/2} \frac{Q_2 S_2}{Q_1 S_1} = \prod_i^{3n-6} \left[\frac{\nu_{2i}}{\nu_{1i}} \ell^{\frac{hc(\nu_{1i} - \nu_{2i})}{2\kappa T}} \frac{1 - \ell^{\frac{-hc\nu_{1i}}{\kappa T}}}{1 - \ell^{\frac{-hc\nu_{2i}}{\kappa T}}}\right] \tag{17}$$

Defining f as

$$f = \prod_j^n \left[\frac{m_{1j}}{m_{2j}}\right]^{3/2} \frac{Q_2}{Q_1}$$

and u_i as

$$u_i = \frac{hc\nu_i}{\kappa T}$$

and

$$u_{1i} = u_{2i} + \Delta u_i$$

$$u_{2i} \equiv u_i$$

leads to the expression

$$\frac{S_2}{S_1}f = \prod_{i}^{3n-6}\left[\frac{u_i}{u_i+\Delta u_i}\; e^{\frac{\Delta u_i}{2}}\; \frac{1-e^{-(u_i+\Delta u_i)}}{1-e^{-u_i}}\right] \qquad (18)$$

in which u_i refers to the heavier isotope.

Taking logarithms of both sides of Equation 18 gives

$$\ln f + \ln\frac{S_2}{S_1} = \sum_{i}^{3n-6}\left[\ln\frac{u_i}{u_i+\Delta u_i} + \frac{\Delta u_i}{2} + \ln\frac{1-e^{-(u_i+\Delta u_i)}}{1-e^{-u_i}}\right] \qquad (19)$$

$$= \sum_{i}^{3n-6}\left[-\ln\left[1+\frac{\Delta u_i}{u_i}\right] + \frac{\Delta u_i}{2} + \ln\frac{1-e^{-(u_i+\Delta u_i)}}{1-e^{-u_i}}\right] \qquad (20)$$

For all cases in which $\Delta u_i \ll 1$, i.e. all cases except those involving the isotopes of hydrogen,

$$\ln f + \ln \frac{S_2}{S_1} = \sum_i^{3n-6} \left[-\frac{\Delta u_i}{u_i} + \frac{\Delta u_i}{2} - \ln \left[\frac{e^{u_i} - 1}{e^{u_i} e^{\Delta u_i} - 1} \right] \right] \quad (21)$$

$$= \sum_i^{3n-6} \left[-\frac{\Delta u_i}{u_i} + \frac{\Delta u_i}{2} + \ln \left[\frac{e^{u} + \Delta u_i - 1}{e^{u_i} - 1} \right] \right] \quad (22)$$

$$= \sum_i^{3n-6} \left[-\frac{\Delta u_i}{u_i} + \frac{\Delta u_i}{2} + \ln \left[1 + \frac{\Delta u_i}{e^{u_i} - 1} \right] \right] \quad (23)$$

$$= \sum_i^{3n-6} \left[\left[-\frac{1}{u_i} + \frac{1}{2} + \frac{1}{e^{u_i} - 1} \right] \Delta u_i \right] \quad (24)$$

$$= \sum_i^{3n-6} G(u_i)\, \Delta u_i \quad (25)$$

where $G(u_i) = \frac{1}{2} - \frac{1}{u_i} + \frac{1}{e^{u_i} - 1}$

Thus, approximately,

$$\frac{S_2}{S_1} f = \prod_i^{3n-6} (1 + G(u_i)\, \Delta u_i) \quad (26)$$

and

$$\frac{S_2}{S_1}\oint = 1 + \sum_{i}^{3n-6} G(u_i)\,\Delta u_i \qquad (27)$$

The Term $Q_1^{\ddagger}/Q_2^{\ddagger}$

In an analogous manner, it can be shown that

$$\frac{Q_2^{\ddagger}}{Q_1^{\ddagger}} \prod_{j}^{n} \left[\frac{m_{1_j}}{m_{2_j}}\right]^{3/2} \frac{S_2^{\ddagger}}{S_1^{\ddagger}} = \prod_{i}^{3n-6} \frac{u_{2_i}^{\ddagger}}{u_{1_i}^{\ddagger}} \prod_{i}^{3n-7} \ell^{\frac{\Delta u_i^{\ddagger}}{2}} \frac{1-\ell^{-u_{1_i}^{\ddagger}}}{1-\ell^{-u_{2_i}^{\ddagger}}} \qquad (28)$$

One degree of freedom is missing in the second product term in the right-hand side of Equation 28. This is the decomposition made, and is an imaginary vibration whose 'u' is designated u_L. Thus

$$\frac{S_2^{\ddagger}}{S_1^{\ddagger}}\oint^{\ddagger} = \frac{\nu_{2_L}^{\ddagger}}{\nu_{1_L}^{\ddagger}} \prod_{i}^{3n-7} \frac{u_{2_i}^{\ddagger}}{u_{1_i}^{\ddagger}}\, \ell^{\frac{\Delta u_i^{\ddagger}}{2}} \frac{1-\ell^{-u_{1_i}^{\ddagger}}}{1-\ell^{-u_{2_i}^{\ddagger}}} \qquad (29)$$

or,

$$\frac{S_2^{\ddagger}}{S_1^{\ddagger}}\oint^{\ddagger} = \frac{\nu_{2_L}^{\ddagger}}{\nu_{1_L}^{\ddagger}} \left[1 + \sum_{i}^{3n-7} G(u_i^{\ddagger})\,\Delta u_i^{\ddagger}\right] \qquad (30)$$

The Original Bigeleisen Equation

Dividing Equation 27 by Equation 30 gives

$$\frac{k_1 S_2 S_1^{\ddagger}}{k_2 S_1 S_2^{\ddagger}} = \frac{\nu_{1_L}^{\ddagger}}{\nu_{2_L}^{\ddagger}} \left[\frac{1 + \sum_i^{3n-6} G(u_i)\Delta u_i}{1 + \sum_i^{3n-7} G(u_i^{\ddagger})\Delta u_i^{\ddagger}} \right] \tag{31}$$

So, approximately,

$$\frac{k_1 S_2 S_1^{\ddagger}}{k_2 S_1 S_2^{\ddagger}} = \frac{\nu_{1_L}^{\ddagger}}{\nu_{2_L}^{\ddagger}} \left[1 + \sum_i^{3n-6} G(u_i)\Delta u_i - \sum_i^{3n-7} G(u_i^{\ddagger})\Delta u_i^{\ddagger} \right] \tag{32}$$

The Tunnelling Correction (45)

If the potential along the reaction path through the transition state is approximated by the parabola

$$V = V_o - ax^2$$

the tunnelling factor, τ, becomes

$$\tau = 1 + \frac{1}{24}\left[\frac{h}{T}\sqrt{\frac{a}{m}} \right]^2 \tag{33}$$

$$= 1 + \frac{1}{24}\left| u_L^{\ddagger} \right|^2 \tag{34}$$

and the isotope effect due to tunnelling becomes

$$\frac{\tau_1}{\tau_2} = 1 + \frac{1}{24}\Delta\left|u_i^{\ddagger}\right|^2 \tag{35}$$

and Equation 32 becomes

$$\frac{k_1 S_2 S_1^{\ddagger}}{k_2 S_1 S_2^{\ddagger}} = \frac{\upsilon_{1_i}^{\ddagger}}{\upsilon_{2_i}^{\ddagger}}\left[1 + \sum_{i}^{3n-6} G(u_i)\,\Delta u_i - \sum_{i}^{3n-7} G(u_i^{\ddagger})\,\Delta u_i^{\ddagger}\right] \cdot \left[1 + \frac{1}{24}\Delta\left|u_i^{\ddagger}\right|\right] \tag{36}$$

The Modified First Quantum Correction

Expansion of G(u) in powers of u gives u/12 as the first term.

Thus, for small values of u_i and Δu_i, Equation 27 becomes

$$\frac{S_2}{S_1}\int = 1 + \sum_{i}^{3n-6}\frac{u_i}{12}\Delta u_i \tag{37}$$

$$= 1 + \sum_{i}^{3n-6}\frac{u_{1_i}^2 - u_{2_i}^2}{24} \tag{38}$$

The sum rule (46) states that

$$4\pi^2 \sum_{i}^{3n-6} \left[\nu_{1i}^2 - \nu_{2i}^2 \right] = \sum_{j}^{3n} \left[\frac{1}{m_{1_j}} - \frac{1}{m_{2_j}} \right] a_{jj} \qquad (39)$$

Thus

$$\frac{S_2}{S_1}\int = 1 + \frac{1}{24}\left[\frac{Kc}{\kappa T}\right]^2 \sum_{j}^{3n} \left[\frac{1}{m_{1_j}} - \frac{1}{m_{2_j}} \right] a_{jj} \qquad (40)$$

Equation 27 can be rewritten

$$\frac{S_2}{S_1}\int = 1 + \sum_{i}^{3n-6} G(u_i)\,\Delta u_i \cdot \frac{12}{u_i} \cdot \frac{u_i}{12} \qquad (41)$$

$$= 1 + \sum_{i}^{3n-6} \gamma_i \frac{u_i}{12} \Delta u_i \qquad (42)$$

$$\text{where } \gamma_i = \frac{12 G(u_i)}{u_i}$$

and thus

$$\frac{S_2}{S_1}\int = 1 + \sum_{i}^{3n-6} \frac{\gamma_i}{24} \left[u_{1_i}^2 - u_{2_i}^2 \right] \qquad (43)$$

Since the quantity γ does not vary rapidly with u , it is possible to define a convenient quantity, γ, such that

$$\frac{S_2}{S_1}f = 1 + \bar{\gamma}\sum_{i}^{3n-6}\left[\frac{u_{1i}^2 - u_{2i}^2}{24}\right] \tag{44}$$

Equation 40 can now be rewritten

$$\frac{S_2}{S_1}f = 1 + \frac{1}{24}\left[\frac{\hbar c}{\kappa T}\right]^2 \bar{\gamma}\sum_{j}^{3n}\left[\frac{1}{m_{1j}} - \frac{1}{m_{2j}}\right]a_{jj} \tag{45}$$

Because u_L^* is small, it is approximately true that

$$\frac{1}{24}\Delta\left|u_L^{\ddagger}\right|^2 = \frac{u_L^*}{12}u_L^* = G(u_L^{\ddagger})\Delta u_L^{\ddagger}$$

and Equation 36 then becomes Equation 46:

$$\frac{k_1 S_2 S_1^*}{k_2 S_1 S_2^{\ddagger}} = \frac{\nu_{1L}^{\ddagger}}{\nu_{2L}^{\ddagger}}\left[1 + \sum_{i}^{3n-6} G(u_i)\Delta u_i - \sum_{i}^{3n-6} G(u_i^{\ddagger})\Delta u_i^{\ddagger}\right] \tag{46}$$

$$= \frac{\nu_{1L}^{\ddagger}}{\nu_{2L}^{\ddagger}}\left[1 + \frac{\bar{\gamma}}{24}\sum_{i}^{3n-6}(u_{1i}^2 - u_{2i}^2) - \frac{\bar{\gamma}^*}{24}\sum_{i}^{3n-6}(u_{1i}^{\ddagger 2} - u_{2i}^{\ddagger 2})\right] \tag{47}$$

$$= \frac{\nu_{1_L}^{\ddagger}}{\nu_{2_L}^{\ddagger}}\left[1 + \frac{\bar{\gamma}}{24}\left[\frac{\hbar c}{\kappa T}\right]^2 \sum_{j}^{3n}\left[\frac{1}{m_{1j}} - \frac{1}{m_{2j}}\right] a_{jj} - \frac{\bar{\gamma}^{\ddagger}}{24}\left[\frac{\hbar c}{\kappa T}\right]^2 \sum_{j}^{3n}\left[\frac{1}{m_{1j}} - \frac{1}{m_{2j}}\right] a_{jj}\right] \qquad (48)$$

and if $\bar{\gamma} = \bar{\gamma}^{\ddagger}$

$$\frac{k_1 S_2 S_1^{\ddagger}}{k_2 S_1 S_2^{\ddagger}} = \frac{\nu_{1_L}^{\ddagger}}{\nu_{2_L}^{\ddagger}}\left[1 + \frac{\bar{\gamma}}{24}\left[\frac{\hbar c}{\kappa T}\right]^2 \sum_{j}^{3n}\left[\frac{1}{m_{1j}} - \frac{1}{m_{2j}}\right]\left[a_{jj} - a_{jj}^{\ddagger}\right]\right] \qquad (49)$$

Equation 49 is the so-called 'gamma-bar approximation'.

APPENDIX C

The Modified Schmidt Decarboxylation

A. Introduction

For reasons outlined elsewhere in this thesis, it was decided at the outset of the present work that all isotopic abundances were to be determined mass-spectrometrically. This approach requires that a method be found for the isolation, in high yield and purity, of the carbon atom in the reactant (and in the product) constituting the reaction site, in the form of carbon dioxide. For the benzyl chlorides and benzyl methyl ethers employed in this study, oxidation to the benzoic acid followed by decarboxylation is the method of choice.

For the decarboxylation step a reaction discovered by K.F. Schmidt (49) was examined for suitability. The Schmidt decarboxylation, as it is called, has certain advantages, namely experimental simplicity, ready adaptability to use on a semi-micro scale (50), and a complete absence of that anathema of carbon isotope effect work, side reactions producing carbon dioxide.

While yields of both amine and carbon dioxide are frequently almost quantitative, it has been observed (51) that benzoic acids bearing electron-withdrawing substituents give poor yields. The reaction rates are too slow for practical purposes in these cases.

Since certain of the benzoic acids obtained in the present work were so substituted, an attempt was made to improve the reaction to include such acids as practical substrates.

B. The 'Modified' Reaction

The presence of a strong mineral acid is essential for the Schmidt decarboxylation. Concentrated sulphuric acid is most commonly used, and frequently serves as the solvent. Dilution of the reaction mixture with inert organic solvents is also practiced, although this technique seems to have little effect on yields. Neither method is of value when the substrate is an electronegatively substituted benzoic acid.

Although the mechanism of this decarboxylation has not yet been established unequivocally, it is highly probable that the reaction proceeds along either of the two following pathways:

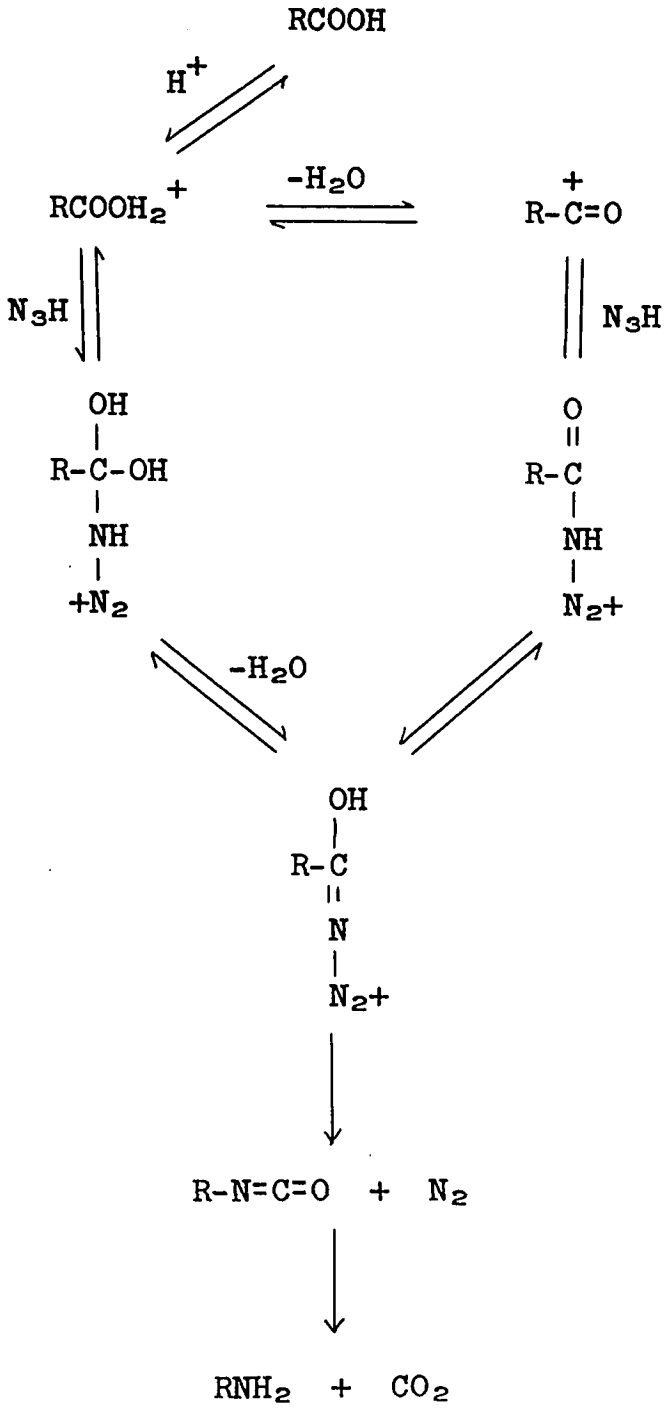

The identity of the rate-controlling step in this scheme has been the subject of some controversy (52).

It would appear, however, that an increase in the acidity of the reaction medium should lead to faster reaction rates. An attempt was made, therefore, to bring about a satisfactory decarboxylation in a more acidic solvent, namely '100% sulphuric acid.' p-Nitrobenzoic acid gives nearly quantitative yields of p-nitroaniline and carbon dioxide under these conditions.

Because of this observation, a series of electronegatively substituted benzoic acids were subjected to the modified Schmidt reaction. The results appear in the accompanying table.

Only 3,5-dinitrobenzoic acid among those tested proved resistant to the new conditions. A further increase, however, in the acidity of the medium, i.e. the use of '20% oleum,' led to nearly quantitative yields in this case as well.

Substituent	Sulphuric Acid Concentration				
	96%	100%		20% oleum	
	% Yields				
	$BaCO_3$	$BaCO_3$	Aniline	$BaCO_3$	Aniline
H	90.5	96.5	67 a	-	-
4-OMe	91.8	96.5	0 a	-	-
4-F	71.7	99.5	92	-	-
4-Cl	51.3	98.0	99	-	-
4-Br	50.3	97.5	96	-	-
4-CN	7.6	100	73 b	-	-
4-CF_3	-	97.4	41 c	-	-
4-NO_2	8.1	99.0	99	-	-
3-NO_2	6.1	98.3	100	-	-
3,5-di-NO_2	-	3.2	-	97.6	82

a. Sulphonation would be expected

b. Isolated as p-aminobenzamide

c. Isolated as the N-acetyl derivative

APPENDIX D

THE REACTION OF BROMIDE ION WITH α-TOLUENESULPHONYL BROMIDES

A novel reaction of α-toluenesulphonyl bromides, i.e. their decomposition to yield benzyl bromides and sulphur dioxide upon treatment with alkylammonium bromides, was discovered by Prof. J.F. King and Dr. D.J.H. Smith in this department (54).

$$C_6H_5CH_2SO_2Br \xrightarrow{Br^-} C_6H_5CH_2Br + SO_2 \qquad (1)$$

The reaction proceeds readily and quantitatively in inert solvents such as methylene chlorate and acetonitrile.

Kinetic measurements showed the reaction to be clearly first order in the sulphonyl bromide but only approximately so in the bromide salt. It was believed that the reaction was bimolecular, and that the deviation from pure second-order kinetics was due to ionic association in the non-polar solvents used.

The Hammett plot was found to be non-linear, a characteristic commonly observed in the S_N2 reactions of

benzyl halides (55,56). Furthermore, (R)-α-toluenesulphonyl bromide gave, under these conditions, mainly the inverted product.

The mechanism proposed involved simultaneous bimolecular nucleophilic displacement and concerted fragmentation as shown in Equation 2:

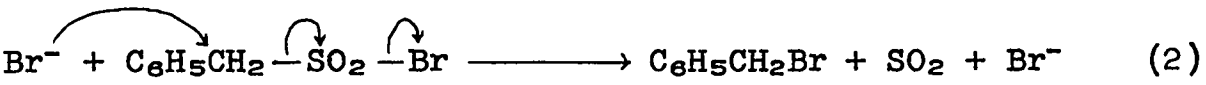

$$Br^- + C_6H_5CH_2{-}SO_2{-}Br \longrightarrow C_6H_5CH_2Br + SO_2 + Br^- \qquad (2)$$

Overall, this reaction is more complex than that of an alkoxide ion with a benzyl halide:

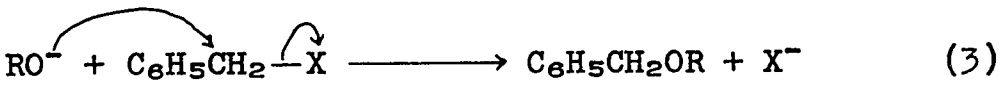

$$RO^- + C_6H_5CH_2{-}X \longrightarrow C_6H_5CH_2OR + X^- \qquad (3)$$

Considered only in terms of what is occurring at the benzylic carbon atom, however, both reactions are simple nucleophilic displacements.

Because of this similarity, it was decided to undertake, in collaboration with Dr. Smith, a carbon-13 kinetic isotope effect study of the α-toluenesulphonyl bromide-bromide ion reaction similar to that reported in the body of this thesis for the benzyl chloride-alkoxide ion reaction.

Kinetic measurements and isotope effect runs were carried out by Dr. Smith, who subsequently supplied the author with samples of the products of both 15% and 100%

reaction. All samples so supplied were benzyl bromides. Degradations, isotopic analyses and kinetic isotope effect calculations were performed by the author.

The experimental values obtained are shown in Table IX.

TABLE IX

The Bromide Ion - α-Toluenesulphonyl Bromide Reaction

Substituent	Run	k^{12}/k^{13}
H	SI1	1.0337
	SI2	1.0369
	SI5	1.0335
	SI6	1.0367
	Average	1.0362 ±0.0016
m-Cl	SII1	1.0452
	SII2	1.0454
	Average	1.0453
p-Cl	SIII1	1.0293
	SIII2	1.0321
	SIII3	1.0322
	Average	1.0312 ±0.0013
p-NO_2	SIV1	1.0534
	SIV2	1.0550
	SIV3	1.0548
	Average	1.0544 ±0.0007
m-NO_2	SV1	1.0414
	SV2	1.0401
	SV3	1.0416
	Average	1.0414 ±0.0008

While the results reported in the above table do not necessarily validate the mechanism shown in Equation 2, they are certainly consistent with such a mechanism. Their magnitude is in the range reported (57,58,59) for bimolecular processes involving benzylic systems (see also Chapter III of this thesis).

The effect of substituents on the kinetic isotope effect for the reaction can be seen clearly in Table IX, and can be related to polar effects as summarized in Table X.

TABLE X

Polar Effects and Kinetic Isotope Effects in the α-Toluenesulphonyl Bromide-Bromide Ion Reaction

Substituent	Inductive Effect	Resonance Effect	k^{12}/k^{13}
p-Cl	Electron withdrawl	Electron release	1.031
m-Cl	Electron withdrawl	-	1.045
m-NO_2	Electron withdrawl	-	1.041
p-NO_2	Electron withdrawl	Electron withdrawl	1.054

The substituent effect parallels that observed for the bimolecular benzyl chloride-alkoxide ion reaction, i.e. electron-withdrawing substituents increase the kinetic isotope effect.

The substituent effect can be discussed usefully in terms of the simple, linear, three-center transition state

Br-------C-------S

II

The Swain-Thornton rule (34) predicts, (as one would intuitively expect) that a decreased electron supply at the central carbon atom of this transition state (such as would be induced by the introduction of an electron-withdrawing substituent) would tend to shorten its carbon-bromine and carbon-sulphur 'bonds'. The Bigeleisen theory of kinetic isotope effects (see Appendix B) predicts, for this transition state model, a smaller isotope effect on shortening these 'bonds' in this way. Such a prediction is contradicted by experimental observation.

The situation is obviously more complex than is suggested by Model II. No account, for instance, has been taken of resonance interaction between the aromatic ring and the benzylic carbon atom. If it is assumed that such an interaction (with its concomittant ring-benzylic carbon bond

shortening) is involved in the transition state for this reaction, introduction of an electron-withdrawing substituent would lengthen the ring-benzylic carbon bond while shortening the carbon-bromine and carbon-sulphur 'bonds'. It has been shown (see the Discussion of Results in this thesis) that a small change in the ring-benzylic carbon bond length can completely overshadow a much larger change in the opposite direction in the two other 'bonds'. It is proposed here that such interaction is indeed involved in the transition state for this reaction. This proposal is in accord with the conclusions drawn for the benzyl chloride-alkoxide ion reaction discussed earlier.

REFERENCES

1. H.N. McCoy and W.H. Ross, J. Am. Chem. Soc. 29, 1968 (1907).

2. F. Soddy, J. Chem. Soc. 99, 72 (1910).

3. F. Lindeman, Phil. Mag. 37, 523 (1919).

4. F. Lindeman, Phil. Mag. 38, 173 (1919).

5. H.C. Urey, F.G. Brickwedde and G.M. Murphy, Phys. Rev. 39, 164 (1932).

6. H.C. Urey, F.G. Brickwedde and G.M. Murphy, Phys. Rev. 40, 1 (1932).

7. H.S. King and R.T. Birge, Nature 124, 127 (1929).

8. S.M. Naude, Phys. Rev. 35, 130 (1930).

9. S.M. Naude, Phys. Rev. 36, 323 (1930).

10. W.F. Giaque and H.L. Johnston, J. Am. Chem. Soc. 51, 1346 (1929).

11. W.F. Giaque and H.L. Johnston, J. Am. Chem. Soc. 51, 3528 (1929).

12. E.R. Washburn and H.C. Urey, Proc. Natl. Acad. Sci. 18, 496 (1932).

13. H.C. Urey and D. Rittenberg, J. Chem. Phys. 1, 137 (1933).

14. D. Rittenberg, W. Bleakney and H.C. Urey, J. Chem. Phys. 2, 48 (1934).

15. D. Rittenberg and H.C. Urey, J. Am. Chem. Soc. 56, 1885 (1934).

16. H.C. Urey and L.J. Graef, J. Am. Chem. Soc. 57, 321 (1935).

17. L.H. Weber, M.H. Wahl and H.C. Urey, J. Chem. Phys. 3, 129 (1935).

18. J. Bigeleisen and G.M. Mayer, J. Chem. Phys. 15, 261 (1947).

19. K. Wiberg, Physical Organic Chemistry, John Wiley and Sons, Inc., New York (1964).

20. S. Glasstone, K.J. Laidler and H. Eyring, The Theory of Rate Processes, McGraw-Hill, New York (1941).

21. F.H. Westheimer, Chem. Rev. 61, 265 (1961).

22. E.D. Hughes, C.K. Ingold and C.S. Patel, J. Chem. Soc. 1933, 526.

23. J.L. Gleave, E.D. Hughes and C.K. Ingold, J. Chem. Soc. 1935, 236.

24. V. Gold, J. Chem. Soc. 1956, 4633.

25. P. Walden, Ber. 27, 133 (1896).

26. E. Fisher, Ber. 39, 2893 (1906).

27. E.D. Hughes, F. Juliusberger, S. Masterman, B. Topley and J. Weiss, J. Chem. Soc. 1935, 1525.

28. W.A. Cowdrey, E.D. Hughes, T.P. Nevell and C.L. Wilson, J. Chem. Soc. 1938, 209.

29. W.A. Cowdrey, E.D. Hughes, C.K. Ingold, S. Masterson and A.D. Scott, J. Chem. Soc. 1937, 1252.

30. H.R. Snyder and J.H. Brewster, J. Am. Chem. Soc. 71, 291 (1949).

31. S. Siegel and A.F. Graefe, J. Am. Chem. Soc. 75, 4521 (1953).

32. S. Winstein, D. Darwish and H.J. Holness, J. Am. Chem. Soc. 78, 2915 (1956).

33. G.S. Hammond, J. Am. Chem. Soc. 77, 334 (1955).

34. C.G. Swain and E.R. Thornton, J. Am. Chem. Soc. 84, 817 (1962).

35. E.R. Thornton, Solvolysis Mechanisms, Ronald Press Co., New York (1964).

36. E.R. Thornton, J. Am. Chem. Soc. 89, 2915 (1967).

37. W.H. Stevens and R.W. Attree, J. Chem. Phys. 18, 574 (1950).

38. Dictionary of Organic Compounds, Eyre and Spottiswoode, London (1965).

39. M. Calvin, C. Heidelberger, J.C. Reid, B.M. Tolbert and P.E. Yankwich, Isotopic Carbon, J. Wiley and Sons, Inc., New York (1949).

40. L. Melander, Isotope Effects on Reaction Rates, Ronald Press, New York (1960).

41. R.M. Badger, J. Chem. Phys. 2, 128 (1934).

42. J.F. Bukta, B.Sc. Thesis, U.W.O. (1967).

43. J. Bigeleisen and M. Wolfsberg, J. Chem. Phys. 21, 1972 (1953).

44. J. Bigeleisen, J. Chem. Phys. 17, 675 (1949).

45. J. Bigeleisen and M. Wolfsberg, Advan. Chem. Phys. 1, 15 (1958).

46. M. Wiberg, J. Chem. Phys. 33, 2 (1960).

47. E.P. Wigner, Z. physik. Chem. B19, 903 (1932).

48. J.C. Decius and E.B. Wilson, J. Chem. Phys. 19, 1409 (1951).

49. K.F. Schmidt, Z. angew. Chem. 36, 511 (1923).

50. F.B. Fisher and A.N. Bourns, Can. J. Chem. 39, 1736 (1961).

51. J.B. Stothers and A.N. Bourns, Can. J. Chem. 38, 923 (1960).

52. P. de Mayo, Molecular Rearrangements, Vol. I, Interscience Publishers, New York (1963).

53. A.J. McNamara and J.B. Stothers, Can. J. Chem. 42, 2354 (1964).

54. J.F. King and D.J.H. Smith, J. Am. Chem. Soc. 89, 4803 (1967).

55. C.G. Swain and W.P. Langsdorf, Jr., J. Am. Chem. Soc. 73, 2813 (1951).

56. R.F. Hudson and G. Klopman, J. Chem. Soc. 1962, 1062.

57. J.B. Stothers and A.N. Bourns, Can. J. Chem. 40, 2007 (1962).

58. A. Fry, Pure Appl. Chem. 8, 409 (1964).

59. J.B. Stothers and J. Bron, private communication.

SAMPLE CALCULATION OF KIE

C-Cl transition state 'bond' stretched 35%

$\beta/\alpha = 1$, i.e. $a_{jj}^{\ddagger}(\text{C-O}) = a_{jj}^{\ddagger}(\text{C-Cl})$

$\gamma = 0.850$

$a_{jj}(\text{C-Cl}) = 3.40 \times 10^5$ dynes/cm.

$a_{jj}^{\ddagger}(\text{C-Cl}) = 0.90 \times 10^5$ dynes/cm.

$$\frac{k^{12}}{k^{13}} = \frac{\nu_{1_L}^{\ddagger}}{\nu_{2_L}^{\ddagger}} \left[1 + \frac{\overline{\gamma}}{24} \left[\frac{hc}{\kappa T} \right]^2 \sum \left[\frac{1}{m_{1j}} - \frac{1}{m_{2j}} \right] \left[a_{jj} - a_{jj}^{\ddagger} \right] \right]$$

$$= 1.031 \quad 1 + \frac{0.850}{24} \left[\frac{1.438}{2 \times 298} \right]^2 \left[\frac{1}{12} - \frac{1}{13} \right] \left[\frac{(3.40-1.80)\times 10^5}{1.492 \times 10^{-3}} \right]$$

$$= 1.031(10145)$$

$$= 1.0462$$